Interactions between Control and Process Design under Economic Model Predictive Control

Henrique Oyama
Wayne State University

Helen Durand
Wayne State University, helen.durand@wayne.edu

Recommended Citation

Interactions between Control and Process Design under Economic Model Predictive Control

Henrique Oyama and Helen Durand*,a

a*Department of Chemical Engineering and Materials Science, Wayne State University, Detroit, MI 48202.*

Abstract

Economic model predictive control (EMPC) is a model-based control scheme that integrates process control and economic optimization, which can potentially allow for time-varying operating policies to maximize economic performance. The manner in which an EMPC operates a process to optimize economics depends on the process dynamics, which are fixed by the process design. This raises the question of how process and EMPC designs interact. Works which have addressed process and control design interactions for steady-state operation have sought to simultaneously develop process designs and control law parameters to find the most profitable way to operate a process that is able to prevent process constraints from being violated and to optimize capital costs in the presence of disturbances. Because EMPC has the potential to operate a process in a transient fashion, this work first focuses on how EMPC and process design interact in the absence of disturbances. Using small-scale process examples, we seek to understand the fundamental nature of the interactions between EMPC and process design, including how these interactions can impact computational complexity of the controller and the design procedure. We subsequently utilize the insights gained to suggest controller design variables which might be considered as decision variables for a simultaneous process and control design problem when disturbances are considered.

Key words: Economic model predictive control, model predictive control, process design, process control, chemical processes

*Corresponding author: Tel: +1 (313) 577-3475; E-mail: helen.durand@wayne.edu.

1. Introduction

The incorporation of control design into process design decisions (Kyriakides et al. (2017); Gutierrez et al. (2014); Sanchez-Sanchez and Ricardez-Sandoval (2013); Yuan et al. (2012); Ricardez-Sandoval et al. (2009); Kookos and Perkins (2001); Mohideen et al. (1996a)) at the synthesis/design stage (Skiborowski (2018); Sánchez-Sánchez and Ricardez-Sandoval (2013); Isafiade and Fraser (2010)) of a chemical plant has been recognized as an alternative to the sequential design and steady-state control method to enhance process profitability. The sequential approach addresses the control problem after features of the process have been well established (i.e., control decisions are constrained by the priority given to the process design), which may lead to more expensive or less efficient design selection, and poor dynamic operability in the face of disturbances/uncertainties (Flores-Tlacuahuac and Biegler (2007); Mohideen et al. (1996b); Perkins and Walsh (1996)). However, the recognition that the achievable dynamic performance of a plant is strongly coupled with its process design (e.g., Bansal et al. (2000); Ross et al. (1999); Ziegler and Nichols (1943)) and that profitability of operation is tied both to process design, as well as control design led to the development of procedures for designing processes and controllers simultaneously in a manner that meets process constraints but is optimal with respect to operating objectives such as efficiency/profitability.

The conventional integration of design of processes and control can be performed sequentially via heuristics for process synthesis or simultaneously via, for example, an optimization problem in which the decision variables representing process and control design variables are selected based on metrics such as economic criteria Ricardez-Sandoval et al. (2011). In the literature, evaluating process designs from a controllability perspective has been important for analyzing their dynamic behavior when steady-state operation is desired (Perkins and Walsh (1996); R Vinson and Georgakis (2000)). Operability has also been investigated (i.e., analyzing the extent to which desired outputs can be reached for a given set of inputs Gazzaneo and Lima (2019); Carrasco and Lima (2017)) with respect to process intensification (Moulijn et al. (2008); Skiborowski (2018)), and simultaneous design of processes and controllers has been explored for the selection of regulatory

control structures for chemical processes including ordinary Bansal et al. (2002) and reactive distillation Georgiadis et al. (2002). Tractable methods for attempting to determine control and process designs simultaneously have been a focus of the literature regarding the simultaneous design and control problem (which can be represented as a mixed integer dynamic optimization problem in which the optimal design is selected from a set of alternatives). Examples of methods explored include sequential optimization problems Sakizlis et al. (2004), mixed integer nonlinear programming formulations Flores-Tlacuahuac and Biegler (2005), and back-off approaches with power series expansions Rafiei-Shishavan et al. (2017). These advances are particularly important to enhance profitability and ensure safe operation in the context of increasingly integrated and automated processes Pistikopoulos and Diangelakis (2016); Davis et al. (2015); Christofides et al. (2007) and sustainable manufacturing Rafiei and Ricardez-Sandoval (2020).

The literature addressing the co-design of processes and controllers for chemical systems also encompasses advanced control strategies (e.g., model predictive control or MPC Qin and Badgwell (2003); Rawlings (2000)). Optimization-based approaches for designing processes and model predictive controllers in tandem have explored, for example, including control structure selection in the optimization problem Gutierrez et al. (2014), controllability constraints Francisco et al. (2009) or objective function penalties Brengel and Seider (1992), a stochastic-based worst-case process variability index in which the worst-case scenario is utilized in evaluating the process cost function variability and constraints with a specified probability Bahakim and Ricardez-Sandoval (2014), and an iterative decomposition framework Sanchez-Sanchez and Ricardez-Sandoval (2013).

The above integrated process and control design paradigms have traditionally been developed under the steady-state assumption (i.e., operation at a steady-state point). However, steady-state operation may not necessarily be the optimal operation strategy that maximizes the process economics. Changes in energy costs and variability in product demand and feedstocks require a dynamic process response to maintain or increase competitiveness while respecting social/environmental regulations T. Backx and Marquardt (1998). A literature review of major approaches that add forced dynamic considerations in process design is found in Swartz and Kawajiri (2019); Baldea and Edgar (2018). An EMPC-like policy was utilized in relating average operating costs with storage size and

placement of energy storage units Adeodu and Chmielewski (2018). Economically optimal control actions for simultaneous design and control in the presence of disturbances was explored in Hoffmann et al. (2019). Performance improvement with respect to certain cost-based metrics under a dynamic process operating policy was achieved for periodically operated reactors Budman and Silveston (2008); Douglas (1967); Silveston et al. (1995).

To operate processes such as those for which a periodic operating policy is more profitable than steady-state operation, economic model predictive control (EMPC) Ellis et al. (2014); Huang et al. (2011); Diehl et al. (2011), an optimization-based controller that incorporates an economics-based cost function, may be used to attain optimal economic performance online. However, as processes operated under EMPC may allow time-varying operation (which is very different from traditional steady-state tracking controllers), an understanding of how EMPC design should inform process design decisions (and conversely) is needed to achieve the most economically optimal integrated design. Motivated by the above considerations, this work explores the relationship between EMPC and process design in the absence of disturbances. Section 2 introduces some preliminaries, and Section 3 discusses the concept of simultaneous process and control design, with focus on an EMPC in the controller. Section 3.1 introduces a process example that is used in the remainder of the work for examining interactions between EMPC and process design in the absence of disturbances. Section 3.1.1 begins a series of discussions regarding co-design of processes and EMPC's, including exploring how process designs could be utilized in reducing computation time of decentralized EMPC's and the role of the prediction horizon in dictating EMPC behavior for design analyses. Section 3.1.2 presents some additional discussion regarding the role of design, in the absence of disturbances, in dictating aspects of the time-varying behavior which can be observed in certain cases with EMPC, and Section 4 suggests some controller design variables for EMPC that may be useful for considering simultaneous process and EMPC design when disturbances are considered. Finally, Section 5 concludes the paper.

2. Preliminaries

2.1. Notation

The Euclidean norm of a vector is indicated by $|\cdot|$ and the transpose of a vector x is designated by x^T. R corresponds to the set of real numbers and R_+ represents the set of non-negative real numbers. A continuous function $\alpha : [0, a) \to [0, \infty)$ is said to be of class $\mathcal{K}$ if it is strictly increasing and $\alpha(0) = 0$. Set subtraction is signified by $x \in A/B := \{x \in R^n : x \in A, x \notin B\}$, and a level set of a positive definite function V is denoted by $\Omega_\rho := \{x \in R^n : V(x) \le \rho\}$.

2.2. Class of Systems

We consider the following system of first-order nonlinear ordinary differential equations:

$$\dot{x}(t) = f(x(t), u(t)) \tag{1}$$

where f is a locally Lipschitz nonlinear vector function, $x \in X \in R^n$ is the state vector, and $u \in U \subset R^m$ is the vector of manipulated inputs. The origin is an equilibrium point of the system of Eq. 1 (i.e., $f(0,0) = 0$). We also assume that the system of Eq. 1 is stabilizable in the sense that there exists a control law $h_1(x)$ that can asymptotically stabilize the origin of the closed-loop system of Eq. 1, a positive definite Lyapunov function $V : R^n \to R_+$, and functions $\alpha_j(\cdot)$, $j = 1, \ldots, 4$, of class $\mathcal{K}$, such that the following inequalities are satisfied:

$$\alpha_1(|x|) \le V(x) \le \alpha_2(|x|) \tag{2}$$

$$\frac{\partial V(x)}{\partial x} f(x, h_1(x)) \le -\alpha_3(|x|) \tag{3}$$

$$\left| \frac{\partial V(x)}{\partial x} \right| \le \alpha_4(|x|) \tag{4}$$

$$h_1(x) \in U \tag{5}$$

for all $x \in D \subset R^n$, where D is an open neighborhood of the origin. $\Omega_\rho \subset D \cap X$ is a level set of V referred to as the stability region.

2.3. Economic Model Predictive Control

Economic model predictive control (EMPC) is an optimization-based control design for which the control actions are computed via the following optimization problem:

$$\min_{u(t) \in S(\Delta)} \int_{t_k}^{t_{k+N}} L_e(\tilde{x}(\tau), u(\tau)) \, d\tau \tag{6a}$$

$$\text{s.t.} \quad \dot{\tilde{x}}(t) = f(\tilde{x}(t), u(t)) \tag{6b}$$

$$\tilde{x}(t_k) = x(t_k) \tag{6c}$$

$$\tilde{x}(t) \in X, \ \forall \, t \in [t_k, t_{k+N}) \tag{6d}$$

$$u(t) \in U, \ \forall \, t \in [t_k, t_{k+N}) \tag{6e}$$

where N is called the prediction horizon, and $u(t)$ is a piecewise-constant input trajectory with N pieces, where each piece is held constant for a sampling period with time length Δ. The economics-based stage cost L_e of Eq. 6a is evaluated throughout the prediction horizon using the future predictions of the process states $\tilde{x}$ from the model of Eq. 6b (the model of Eq. 1) initialized from the state measurement at t_k (Eq. 6c). In Eq. 6a, the integration variable is represented by τ to enable the upper and lower limits of the integral to be in terms of time instants. The process constraints of Eqs. 6d-6e are state and input constraints, respectively. A receding or moving horizon implementation strategy is employed, i.e., the optimization problem is solved every Δ time units (at each sampling time t_k) such that the first of the N pieces of the input vector trajectory that is the optimal solution is applied to the process. The optimal solution at t_k is denoted by $u^*(t_i|t_k)$, where $i = k, \ldots, k+N-1$. EMPC that incorporates a quadratic tracking objective function that takes its minimum at the steady-state (i.e., $L_e = x^T Q x + u^T R u$, with Q and R as positive definite matrices), often referred to as model predictive control (MPC), has been widely used in the process industries Qin and Badgwell (2003); Rawlings (2000). Furthermore, mixed state and input constraints can be added to the EMPC in Eq. 6, denoted as follows:

$$g_z(x, u) \in G_z \tag{7}$$

Additional constraints which can be added to the formulation in Eq. 6 to produce a dual-mode formulation of EMPC that takes advantage of the Lyapunov-based controller $h_1(x)$, called

Lyapunov-based EMPC (LEMPC) Heidarinejad et al. (2012), are as follows:

$$V(\tilde{x}(t)) \leq \rho_e, \quad \forall t \in [t_k, t_{k+N}), \quad \text{if } x(t_k) \in \Omega_{\rho_e} \tag{8a}$$

$$\frac{\partial V(x(t_k))}{\partial x} f(x(t_k), u(t_k)) \leq \frac{\partial V(x(t_k))}{\partial x} f(x(t_k), h_1(x(t_k))), \quad \text{if } x(t_k) \in \Omega_\rho / \Omega_{\rho_e} \tag{8b}$$

where $\Omega_{\rho_e} \subset \Omega_\rho$ is a subset of the stability region that makes Ω_ρ forward invariant under the controller of Eqs. 6 and 8.

3. Interactions Between Process Design and EMPC Design

A topic of interest in the process systems engineering literature has been the question of how to optimally design a process in light of the control system's capabilities to reject disturbances and/or track set-point changes. The EMPC presented in Eqs. 6-7, however, does not necessarily drive the process state to an operating steady-state. This raises the question of whether there is anything fundamentally different about how process designs and EMPC designs interact, compared to how process designs and the designs of controllers which track steady-states interact, even in the absence of disturbances.

First, we note a difference between steady-state tracking control and EMPC: there is not much need to discuss how to select controller parameters and process designs together under steady-state operation in the absence of disturbances if the process state is initialized at the steady-state, as then the process is always maintained at the steady-state and any control law should compute the steady-state operating policy. For EMPC, however, this is different. Even if the process is initialized at a steady-state and the EMPC is used to control the process, it may find that a non-steady-state operating policy is preferable to operating at the initial steady-state, meaning that even in the absence of disturbances, there is potential that the process and controller designs interact. For steady-state operating policies, when design and control interact, strategies for simultaneously designing controllers and processes could be used to find the best process/controller parameter combination.

Simultaneous process and control design techniques seek to determine process and controller decision variables mathematically in a manner that allows a process to make the most profit throughout long-term operation. When performed in an optimization-based context, this method selects

optimal values of both discrete/integer variables (e.g., number of trays in a distillation column) and continuous variables (e.g., controller tuning parameters or continuous process design parameters such as reactor size). This simultaneous process and control design framework, incorporating EMPC specifically in this work, would be as follows in the absence of disturbances:

$$\min_{p_{ss}, p_{dv}, c_{dv}} \quad Cost - \int_0^{t_f} R_e(\hat{x}(\tau), u(\tau)) \, d\tau \tag{9a}$$

$$\text{s.t.} \quad u(t) = u^*(t_k|t_k), k = 0, \ldots, (t_f/\Delta - 1), \ \forall\, t \in [t_k, t_{k+1}) \tag{9b}$$

$$\dot{\hat{x}}(t) = f(\hat{x}(t), u(t), p_{ss}, p_{dv}) \tag{9c}$$

$$\hat{x}(t_0) = p_{ss} \tag{9d}$$

$$\hat{x}(t) \in X, \ \forall\, t \in [t_0, t_f) \tag{9e}$$

$$p_{dv} \in H \tag{9f}$$

$$c_{dv} \in A \tag{9g}$$

$$p_{ss} \in O \tag{9h}$$

$$f(x_s, u_s, p_{ss}, p_{dv}) = 0 \tag{9i}$$

$$g_1(\hat{x}, p_{ss}, p_{dv}, c_{dv}) \leqslant 0 \tag{9j}$$

$$u^*(t_k|t_k) = \text{ones}(m, m(N-1))\hat{u}(t_k) \tag{9k}$$

$$\hat{u}(t_k) := \underset{\bar{u}(t) \in S(\Delta)}{\arg\min} \quad -\int_{t_k}^{t_{k+N}} L_e(\tilde{x}(\tau), \bar{u}(\tau)) \, d\tau \tag{10a}$$

$$\text{s.t.} \quad \dot{\tilde{x}}(t) = f(\tilde{x}(t), \bar{u}(t), p_{ss}, p_{dv}) \tag{10b}$$

$$\tilde{x}(t_k) = \hat{x}(t_k) \tag{10c}$$

$$\tilde{x}(t) \in X, \ \forall\, t \in [t_k, t_{k+N}) \tag{10d}$$

$$\bar{u}(t) \in U, \ \forall\, t \in [t_k, t_{k+N}) \tag{10e}$$

$$g_2(\tilde{x}, \bar{u}(t), p_{dv}, c_{dv}) \leqslant 0 \tag{10f}$$

In the above equations, design decision variables such as process decision variables ($p_{dv} \in \mathbb{R}^{n_p}$), controller decision variables ($c_{dv} \in \mathbb{R}^{n_c}$), and a steady-state process condition ($p_{ss} \in \mathbb{R}^{n_s}$), bounded

in the sets H, A, and O, respectively, are solved for. With slight abuse of notation, p_{dv} and $p_{ss} = [x_s \ u_s]^T$, where x_s and u_s are steady-state values of the process states and inputs, respectively, are used as arguments for Eq. 1 to reflect that the dynamic model of Eq. 1 can be rewritten to have its zero value at p_{ss} (Eq. 9i). The role of p_{ss} is that an EMPC requires a state measurement at t_0 to be used (Eq. 6c), and EMPC's are typically operated around a steady-state for stability reasons (e.g., the stability region in Eq. 8 is designed around a steady-state). Therefore, the simultaneous process and EMPC design approach needs to assume an initial condition for the process state and an operating steady-state around which the EMPC will operate the process, and this could be determined via the simultaneous design procedure. In Eq. 9, $Cost$ is the plant capital cost and R_e is the instantaneous process revenue, which in general might be defined differently than the cost function L_e in Eq. 10a. Eq. 9 solves for the design decision variables to maximize the global economic cost function that reflects the long-term profit (defined as the time-integral of the instantaneous revenue obtained by operating the process under EMPC, minus capital costs) in Eq. 9a. Eq. 9i is used as the equality constraints for the identification of the economically-optimal steady-state values (p_{ss}) to start the process under EMPC, and Eq. 9j corresponds to the inequality constraints of combined states and design decision variables in Eq. 9. Although x_s and u_s are entries of the vector p_{ss}, Eq. 9i considers p_{ss} as an argument for consistency with the notation defined in this section. The inputs computed from the EMPC are determined at every sampling time until the end of the time of operation, t_f, over which control and process design is considered, so that new inputs are computed for Eq. 9b t_f/Δ times under the receding horizon strategy of EMPC. Eq. 9b could use the LEMPC formulation defined by Eqs. 6 and 8 if its control features are desired. The process model is given in Eq. 9c and Eq. 10b. The constraints on the states in Eq. 9, referred to as $\hat{x} \in X$, and in Eq. 10, referred to as $\tilde{x} \in X$, are reflected by Eq. 9e and Eq. 10d, respectively, and the constraints on the inputs in Eq. 10 ($\bar{u} \in U$) are delineated by Eq. 10e. $\text{ones}(m, m(N-1))$ represents an $m \times m(N-1)$ matrix with ones in the first m positions for which the row and column numbers are the same, and zeros elsewhere. The vector of inputs in Eq. 9k, $u^*(t_k|t_k)$, defines that the optimal control actions are the first m entries of the vector $\hat{u}(t_k)$ (assumed to be all inputs for the sampling period from t_k to t_{k+1}) obtained from the EMPC in Eq. 10. Thus, $u(t)$ in Eq. 9 refers

to the piecewise constant input trajectory applied to the process in a sample-and-hold fashion. $\hat{x}$ is the vector of predicted states when u is applied to the process model of Eq. 9c. Correspondingly, $\tilde{x}$ is the vector of predicted states when $\bar{u}$ is applied to the process model of Eq. 10b. Because no disturbances/plant-model mismatch are considered in the analyses in this work, we assume that the state predictions are made from an accurate process model. Eq. 10f represents inequality constraints of combined states and decision variables in Eqs. 9-10. Feasibility of the EMPC's in Eqs. 9-10 is important for locating a process/control design combination.

The formulation of Eq. 9-10 is not a novel mathematical construct (i.e., it is a bilevel optimization problem), and we do not in this work seek to address techniques for solving it in a computationally-tractable manner. The goal of this work is instead to seek to elucidate how process and EMPC designs interact in the absence of disturbances. Specifically, we conclude: 1) in the absence of disturbances, a sequential design framework (in which an EMPC is designed before the process) may be sufficient for obtaining appropriate process designs, unless significant simplification is being looked for in computational complexity of the controller itself; 2) a primary advantage of designing processes in light of EMPC designs may be that it is a way to remove steady-state thinking from the design mentality for a controller that fundamentally may not operate a process at steady-state, in much the same way that EMPC allows the computer to figure out the most optimal way to operate a process given the mathematics of the optimization problem to try to prevent traditional steady-state control objectives from fixing the achievable profits with the controller; and 3) in the presence of disturbances, the simultaneous process and EMPC design framework may be of interest to utilize, with an important consideration in that case being the identification of the process and controller design decision variables. The subsequent sections utilize a simple but illustrative process example to address these considerations.

Remark 1. *The receding horizon has the potential to impact the control actions which would be computed by the EMPC over time because as the time horizon shifts one step forward, the inputs computed at a later sampling time may be different than they would have been if predicted at a prior sampling time since a different part of the time of operation is in the controller's horizon and being constrained within the EMPC optimization problem. Including the receding horizon allows the*

10

control actions utilized in finding an optimal design to account for how they would be expected to be computed in the plant.

Remark 2. *We assume a nonlinear/first-principles model for the proposed EMPC formulation rather than a data-driven model. Although this may increase computation time, there is no need to estimate or re-identify the process models when the operating conditions change (e.g., operating around a new steady-state throughout the search for an optimal p_{ss}) as might be required for a data-driven model-based approach. This work also considers the case of no plant-model mismatch, such that a first-principles model is assumed to be available.*

Remark 3. *The simultaneous design and control framework could allow p_{ss}, the optimal steady-state around which operation under EMPC is enforced, to be selected. If an LEMPC is used for the EMPC design, an important consideration is that because Ω_ρ in LEMPC, as well as h_1 and V, are all selected with respect to a given steady-state, allowing p_{ss} to be a decision variable with an LEMPC as the EMPC formulation would require special consideration to ensure that every time p_{ss} is updated in the search for the optimal solution to Eq. 9, the regions Ω_ρ and Ω_{ρ_e}, as well as the functions h_1 and V, are updated when required.*

3.1. Interactions Between Process Design and EMPC Design: Exploring a Simultaneous Process/Control Design Framework without Disturbances

In the following sections, we consider a chemical process consisting of a continuous stirred tank reactor (CSTR) to analyze the conditions under which, even in the absence of disturbances, the simultaneous process/control design framework of Eqs. 9-10 would be beneficial. In the CSTR, the reactant species A is converted to the product B ($A \rightarrow B$) in an irreversible, second-order, exothermic, and liquid-phase reaction. The feed to the reactor contains only the species A in an inert solvent at concentration C_{A0} and temperature T_0, and a jacket is used to provide or remove heat at a rate Q. The inputs C_{A0} and Q, which affect the state variables T (temperature of the CSTR) and C_A (concentration of species A), are determined by an EMPC. The dynamics of the CSTR are as follows, with process parameters listed in Table 1 (Alanqar et al. (2015)):

$$\frac{dC_A}{dt} = \frac{F}{V}(C_{A0} - C_A) - k_0 e^{-\frac{E}{R_g T}} C_A^2 \qquad (11)$$

$$\frac{dT}{dt} = \frac{F}{V}(T_0 - T) - \frac{\Delta H k_0}{\rho_L C_p} e^{-\frac{E}{R_g T}} C_A^2 + \frac{Q}{\rho_L C_p V} \tag{12}$$

where R_g is the ideal gas constant, E is the reaction activation energy, ΔH is the enthalpy of reaction, and k_0 is the pre-exponential constant. The inlet/outlet volumetric flow rate F is assumed fixed, as are the liquid density ρ_L, heat capacity C_p, and liquid volume V. Vectors of deviation variables for the states and inputs from their steady-state values, $C_{As} = 1.22$ kmol/m^3, $T_s = 438.2$ K, $C_{A0s} = 4.0$ kmol/m^3, and $Q_s = 0$ kJ/h, respectively, are $x^T = [x_1\ x_2] = [\bar{C}_A\ \bar{T}]$, where $\bar{C}_A = C_A - C_{As}$ and $\bar{T} = T - T_s$, and $u^T = [u_1\ u_2] = [\bar{C}_{A0}\ \bar{Q}]$, where $\bar{C}_{A0} = C_{A0} - C_{A0s}$ and $\bar{Q} = Q - Q_s$.

Table 1: Parameters for the CSTR model.

Parameter	Value	Unit
V	1	m^3
T_0	300	K
C_p	0.231	kJ/kg·K
k_0	8.46×10^6	m^3/h·kmol
F	5	m^3/h
ρ_L	1000	kg/m^3
E	5×10^4	kJ/kmol
R_g	8.314	kJ/kmol·K
ΔH	-1.15×10^4	kJ/kmol

The structure of the remainder of this section is as follows: we first present a case study which uses the CSTR described above but where a heat exchanger follows the CSTR (i.e., the fluid leaving the CSTR enters a heat exchanger and is cooled in that unit). Through a hypothetical design consideration, analyzed via four subsections, we elucidate the nature of situations in which simultaneous design of a process and EMPC in the absence of disturbances could have value. Subsequently, we utilize a second study in which we focus on controlling the CSTR described above, with various EMPC formulations, to discuss (in three sub-sections) the process and control design implications of the conditions under which time-varying operation may occur under EMPC.

3.1.1. Study 1: Exploring a Simultaneous Process/Control Design Framework via Control of a CSTR Followed by a Heat Exchanger

The first study analyzing whether a simultaneous approach to process and EMPC design is beneficial even in the absence of disturbances adds a counter-current heat exchanger after the CSTR through which the process fluid exiting the reactor flows on the hot side, as shown in Fig. 1, and is cooled as it travels through this unit by a cooling fluid that flows on the cold side of the exchanger. We first present the heat exchanger model and some of the controller constraints, and then present four sub-sections that analyze the benefits and limitations of a simultaneous design approach for this process from different perspectives. Under the assumptions presented in Ogunnaike and Ray (1994); Baldea and Touretzky (2013), the dynamics of the heat exchanger unit are described by the following system of partial differential equations:

$$\frac{\partial T_H}{\partial t} = -v_H \frac{\partial T_H}{\partial z} + \frac{hA_s}{\rho_L A_H C_p}(T_C - T_H) \tag{13}$$

$$\frac{\partial T_C}{\partial t} = v_C \frac{\partial T_C}{\partial z} + \frac{hA_s}{\rho_C A_C C_{pC}}(T_H - T_C) \tag{14}$$

In these equations, T_H is the temperature on the hot side of the counter-current heat exchanger, and T_C is the temperature on the cold side. z represents the distance down the heat exchanger (z = 0 at the outlet of the CSTR, and z = L = 2.5 m at the inlet of the cold side/outlet of the hot side), as shown in Fig. 2. h represents a heat transfer coefficient for the heat transfer between the hot and cold sides through the fluid-solid interfaces of the heat exchanger. A_s is the heat exchange surface area per unit length. ρ_C and ρ_L are the densities of the cold and hot fluids, respectively, and A_H and A_C are the cross-sectional areas through which fluid flows on the hot and cold sides. v_H and v_C represent the magnitudes of the velocities of the fluid flow (calculated as the volumetric flow rate divided by the cross-sectional area) on the hot and the cold sides, respectively, with the assumption that there is no radial variation in the velocity. C_{pC} and C_p are the heat capacities of the cold and hot fluids, respectively. The heat exchanger model parameters are listed in Table 2. The design values assume that the cross-sectional areas of the inner and outer tubes are 0.0082 m^2 and 0.1 m^2, respectively, that the length of the heat exchanger is L = 2.5 m, that the cooling fluid density and heat capacity are those of water (ρ_C = 1000 kg/m^3 and C_{pC} = 4.18 kJ/kg·K), and that
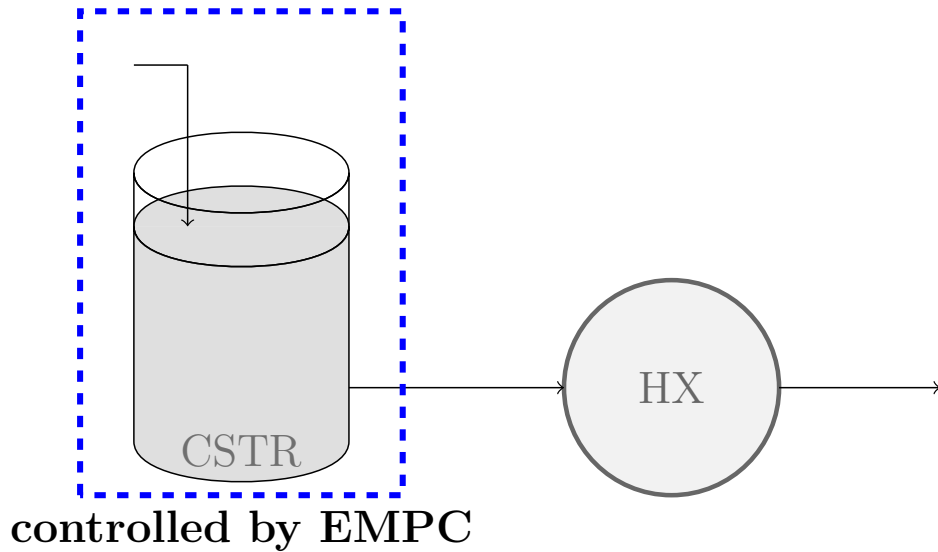
Figure 1: Illustrative chemical process example, where the dashed line represents the system that is controlled by EMPC and "HX" stands for the "heat exchanger".
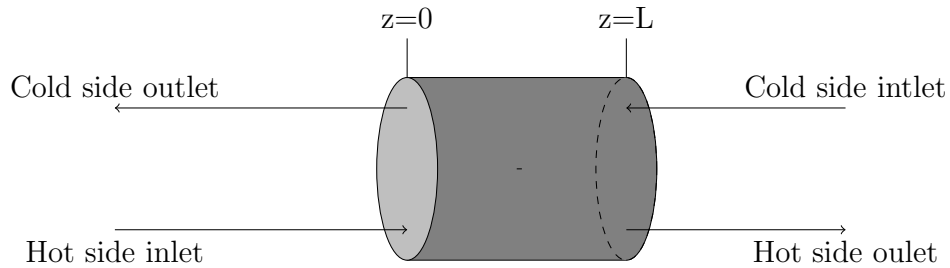
Figure 2: Counter-current heat exchanger.

the heat transfer coefficient is 1080 kJ/h·m^2·K.

We note that the model above (Eqs. 13-14) is a system of partial differential equations instead of first-order nonlinear ordinary differential equations represented by Eq. 1. However, the profiles for T_C and T_H from Eqs. 13-14 can be approximated using the method of lines and discretizing the right-hand side of both partial differential equations in space using finite differences. This forms a system of ordinary differential equations for determining the values of T_C and T_H at every spatial node of the discretized spatial domain of the heat exchanger, making the system of Eqs. 11-12 combined with approximation of the temperature profiles from Eqs. 13-14 a system of the form of Eq. 1.

For this study, the manipulated inputs of the CSTR are adjusted using an EMPC with the control objective being to maximize the production rate of B so that C_{A0} and Q are computed to

14

Table 2: Parameters for the heat exchanger model.

Parameter	Value	Unit
v_H	608	m/h
h	1080	kJ/h·m^2·K
A_s	0.3214	m
ρ_C	1000	kg/m^3
A_C	0.1	m^2
A_H	0.00822	m^2
C_{pC}	4.18	kJ/kg·K

maximize the following objective function:

$$\int_{t_k}^{t_{k+N}} L_e \, d\tau = \int_{t_k}^{t_{k+N}} [k_0 e^{-\frac{E}{RT(\tau)}} C_A(\tau)^2] d\tau \tag{15}$$

In addition, the manipulated input constraints of Eq. 6e were added based on physical requirements $(0.5 \le C_{A0} \le 7.5 \text{ kmol/m}^3$ and $-5.0 \times 10^5 \le Q \le 5.0 \times 10^5 \text{ kJ/h})$.

We now modify the above heat exchanger and EMPC system to explore whether simultaneous determination of process and EMPC parameters may be valuable even in the absence of disturbances. Specifically, we adjust the value of v_c and the EMPC design in the following sections to: A) explore v_c as a process design variable and demonstrate that simultaneous design of the process and EMPC might be valuable in the case that a decentralized control structure is desired to reduce computation time; B) demonstrate that a sequential strategy for determining the process and control designs (in which the EMPC is designed first to incorporate all hard process constraints and the process design is subsequently tuned with knowledge of how that impacts the inputs computed by the EMPC) would be expected to be sufficient for designing a process with a centralized EMPC in the absence of disturbances; C) demonstrate generality of the prior conclusions; and D) provide guidelines for the prediction horizon and sampling period length used in a simultaneous process and EMPC design framework.

3.1.1.1. CSTR and Heat Exchanger Analysis A: Process Design and Controller Computational Complexity. The EMPC described in the above section was used to control the CSTR with Lyapunov-based stability constraints of the form in Eq. 8, designed using a Lyapunov function $V = x^T P x$,

where $P = [1200\ 5; 5\ 0.1]$, and based on x, rather than the states of the full chemical process example because the process states of the CSTR are tied to the heat exchanger temperature profile. Specifically, the fluid temperature exiting the CSTR corresponds to the heat exchanger hot side inlet temperature and, therefore, driving the process states of the reactor to a steady-state will accordingly determine the steady-state temperature profile to be reached in the heat exchanger. The Lyapunov-based controller $h_1(x) = [h_{1,1}(x)\ h_{1,2}(x)]^T$ was developed such that its first component (corresponding to the inlet concentration) was set to $h_{1,1}(x) = 0$ kmol/m³ for simplicity and its second component (corresponding to the heat rate input) was designed using Sontag's formula (Lin and Sontag (1991)):

$$h_{1,2}(x) = \begin{cases} -\frac{L_{\tilde{f}}V + \sqrt{L_{\tilde{f}}V^2 + L_{\tilde{g}_2}V^4}}{L_{\tilde{g}_2}V}, & \text{if } L_{\tilde{g}_2}V \neq 0 \\ 0, & \text{if } L_{\tilde{g}_2}V = 0 \end{cases} \tag{16}$$

where the matrix-valued function that multiplies the input vector in the deviation variable form of Eqs. 11-12 is represented by $\tilde{g}$ (the term $\tilde{g}_2$ constitutes its second column) in Eq. 16, and $\tilde{f}$ denotes the vector-valued function that is only related to the states in the deviation variable form of the CSTR model (Eqs. 11-12). The Lie derivatives of V with respect to $\tilde{f}$ and $\tilde{g}_2$ are represented by $L_{\tilde{f}}V$ and $L_{\tilde{g}_2}V$, respectively. The upper limit of the Lyapunov function was selected to be $\rho = 300$ so that large changes in T would still maintain x within the allowable operating region Ω_ρ, ρ_e was arbitrarily set to 75% of ρ, and the prediction horizon and sampling period were set to $N = 10$ and $\Delta = 0.01$ h, respectively. The simulations were performed for one hour of operation using MATLAB and the function fmincon, with the process states initialized from $x_{init} = [0$ kmol/m³ 0 K$]^T$ and an integration step of 10^{-5} h using the Explicit Euler numerical integration method for the process and for making state predictions within the EMPC. The simulations were performed using a Lenovo model 80XN x64-based ideapad 320 with an Intel(R) Core(TM) i7-7500U CPU at 2.70 GHz, 2904 Mhz, running Windows 10 Enterprise, in MATLAB R2016b. In the optimization problem, the value of u_2 was scaled down by 10^7 to address its larger order of magnitude compared to the other terms.

The resulting trajectories of the states and inputs of the CSTR under the EMPC described above are shown in Figs. 3-4 (the initial guess for the decision variables was the steady-state values of the
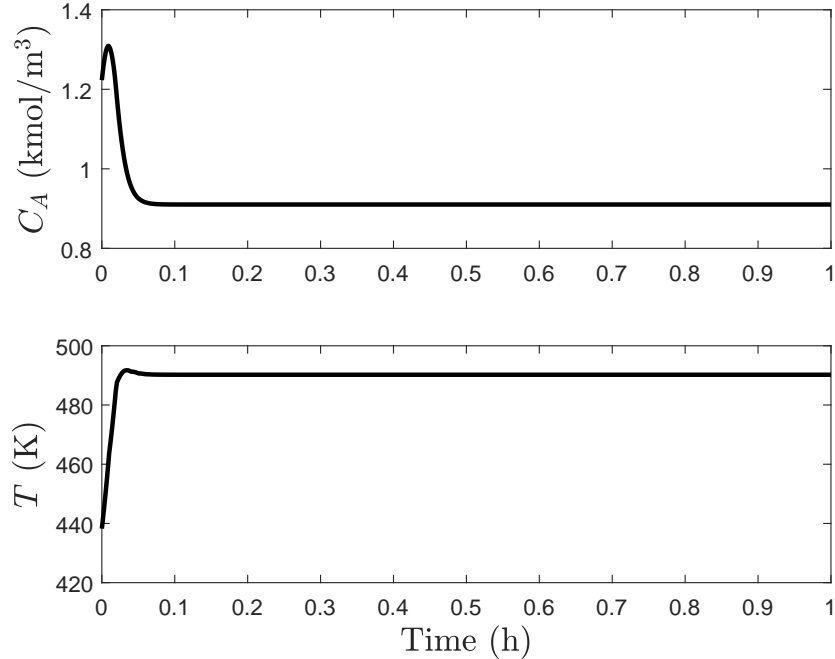
Figure 3: States over one hour of operation for the process of Eqs. 11-12 under the EMPC with Lyapunov-based constraint and input bounds, and optimizing the objective function in Eq. 15.

inputs at each sampling time, with forward finite differences for gradient estimation by fmincon), where the temperature of the stream exiting the CSTR reaches approximately 490.2 K and then remains at this value to maximize profit within the stability region. As the temperature of the fluid in the heat exchanger rises, the temperature of the fluid leaving the cold side of the heat exchanger also rises, and the amount by which it rises depends on the flow rate v_c of the fluid in the cold side of the heat exchanger.

The specific manner in which the value of v_c impacts the temperature out of the heat exchanger on the cold side can be examined via simulations. We first simulate the heat exchanger over time when $v_C = 50$ m/h and the heat exchanger hot side temperature at the z = 0 position is given by the temperature profile from the CSTR under EMPC (Fig. 3). Each side of the heat exchanger was simulated using the method of lines with 19 interior nodes and two boundary nodes in implementing the boundary conditions to solve Eqs. 13-14. At the boundaries z = 0 and at z = L, the forward finite difference and the backward finite difference were implemented, respectively; and between z = 0 and z = L, the centered finite difference method was applied. The boundary conditions are
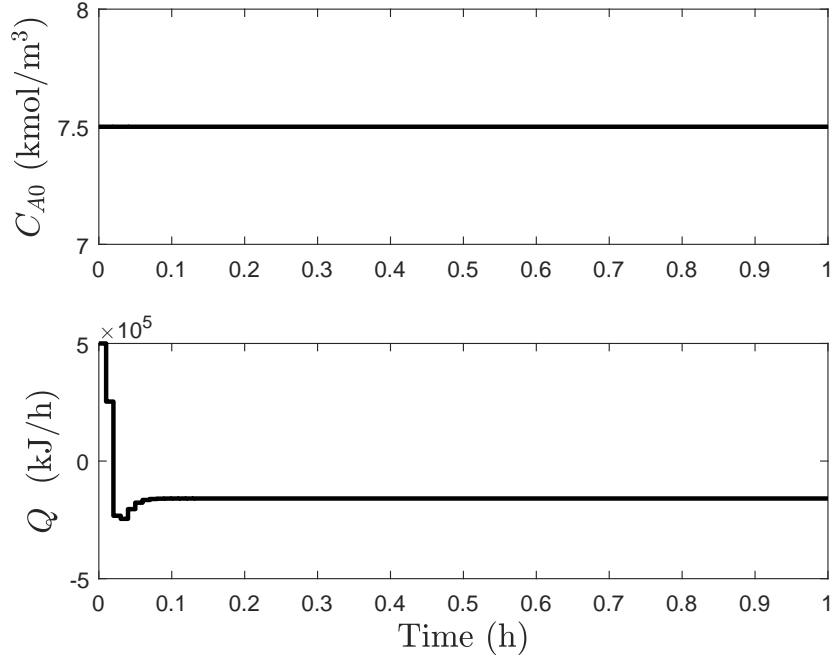
Figure 4: Inputs over one hour of operation for the process of Eqs. 11-12 under the EMPC with Lyapunov-based constraint and input bounds, and optimizing the objective function in Eq. 15.

as follows: the heat exchanger hot side inlet temperature is equal to the temperature of the fluid exiting the CSTR under EMPC (i.e., $T_H = T$ at z = 0) and the heat exchanger cold side inlet temperature is set to 273 K (i.e., $T_C = 273$ K at z = L). To compute the temporal variation in the resulting 21 nodes for each side of the heat exchanger, an integration step of 10^{-5} h was applied. The simulated CSTR in Fig. 3 was presumed to be initially operated at a steady-state corresponding to $C_{As} = 1.22$ kmol/m^3 and $T_s = 438.2$ K and, thus, the heat exchanger is also assumed to be initialized from the steady-state which results when $T_H = T_s$ at z = 0 and $T_C = 273$ K at z = L. These heat exchanger hot and cold side initial temperature profiles were obtained by setting the time derivatives of T_H and T_C in Eqs. 13-14 to 0, and discretizing the spatial domain via finite differences with 19 interior nodes and two boundary nodes (for the interior nodes, centered finite difference approximations were applied; and at z = 0 and z = L positions, forward and backward finite differences were implemented, respectively), resulting in a system of linear algebraic equations that are then solved in MATLAB using the "\" operator. Fig. 5 (top plot) shows the heat exchanger hot and cold side steady-state temperature profiles.

18
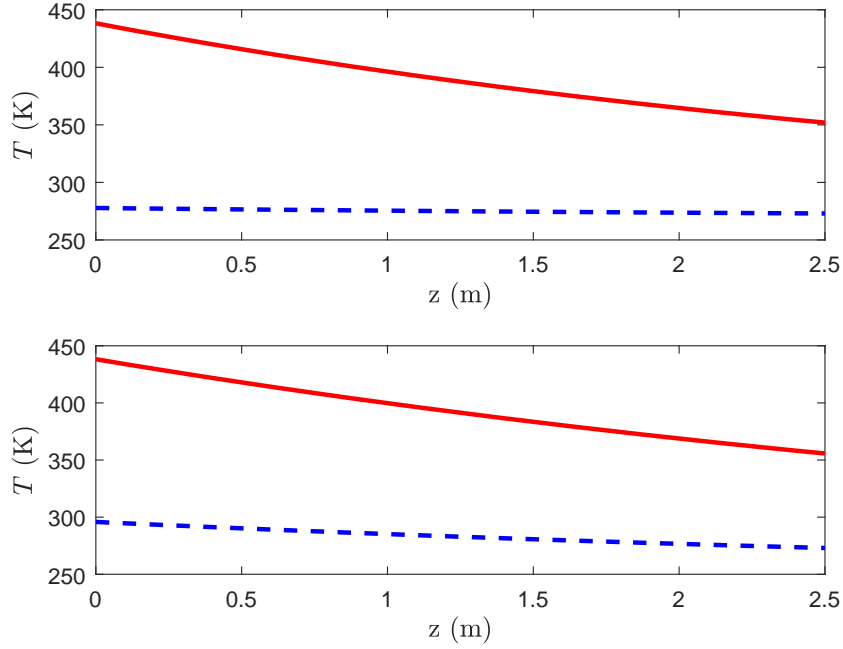
Figure 5: Steady-state temperature profile of the heat exchanger using $v_C = 50$ m/h (top plot) and using $v_C = 10$ m/h (bottom plot), where the solid line represents the temperature profile along the hot side of the heat exchanger and the dashed line represents the temperature profile along the cold side.

The hot and cold side temperature profiles at the z = 0 position of this heat exchanger over time are presented in Fig. 6. We can observe that although there is a large temperature change on the hot side of the heat exchanger (about 50 K) due to the control of the CSTR using EMPC to maximize the production rate of B over one hour of operation, there is only a small change in temperature on the cold side (less than 2 K) over time. This indicates that a process design decision has impacted the effect of the EMPC's control actions on the cold side of the heat exchanger (the change in the temperature on the cold side of the heat exchanger was related to the cooling fluid flow rate).

In contrast, when $v_C = 10$ m/h with all other process parameters defined according to Tables 1-2 and the same hot side temperature at the z = 0 position from the CSTR under EMPC (Fig. 3), changes in the temperature on the hot side of the heat exchanger have a greater effect on the outlet temperature of the heat exchanger cold side. Here, the initial steady-state of the CSTR establishes the initial steady-state profile in the heat exchanger in the bottom plot of Fig. 5 (different from that in the top plot of Fig. 5 when $v_C = 50$ m/h). Starting from this initial steady-state condition,
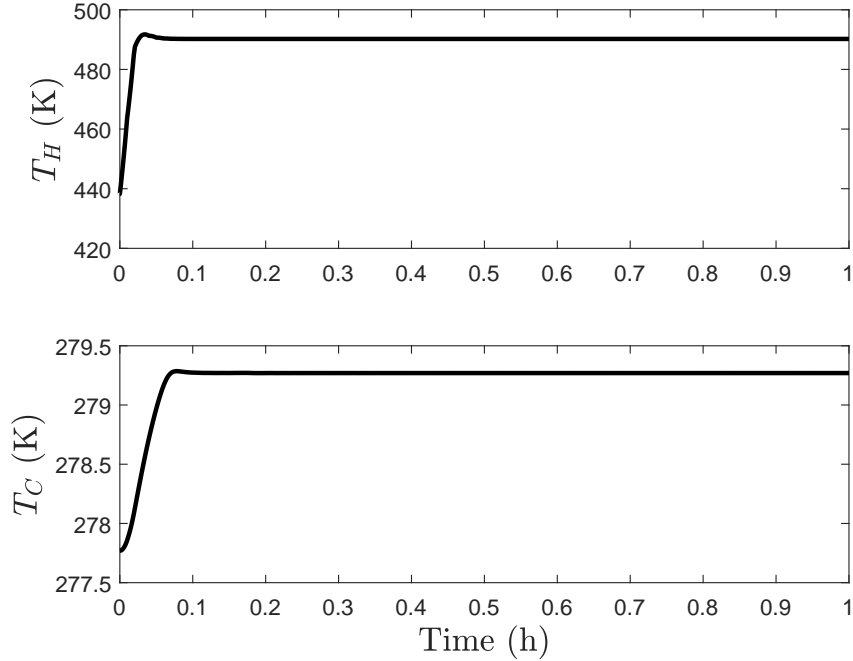
Figure 6: Hot side and cold side temperature profiles of the heat exchanger at the z = 0 position over time using v_C = 50 m/h and with the same inputs from EMPC as used to generate Fig. 3.

with the same temperature profile from the CSTR under the EMPC at the inlet of the hot side of the heat exchanger as in Fig. 6, the cold side temperature profile at the z = 0 position over one hour of operation in Fig. 7 was obtained using the method of lines using v_C = 10 m/h. The lag in the change in temperature on the cold side compared to that on the hot side and the small temperature oscillation observed around 0.3 - 0.5 h on the cold side in Fig. 7 occurs due to a combination of process design parameters (the cooling fluid selection, cooling fluid flow rate, and the counter-current nature of the flow). Specifically, the larger cooling fluid heat capacity on the cold side compared to the hot side causes a larger amount of heat to be absorbed by the material on the cold side in order to change its temperature than on the hot side (and, therefore, the response of the cold side temperature to a change in temperature on the hot side is "delayed" in Fig. 7). Additionally, with the lower cooling fluid flow rate than in the bottom plot of Fig. 6, the impact of the peak in the temperature profile in the hot side of the heat exchanger in Fig. 6 has a greater impact on the cold side temperature profile than when v_c = 50 m/h, and the fluid on the cold side takes a longer period of time to traverse the heat exchanger than in the bottom plot of Fig. 6.
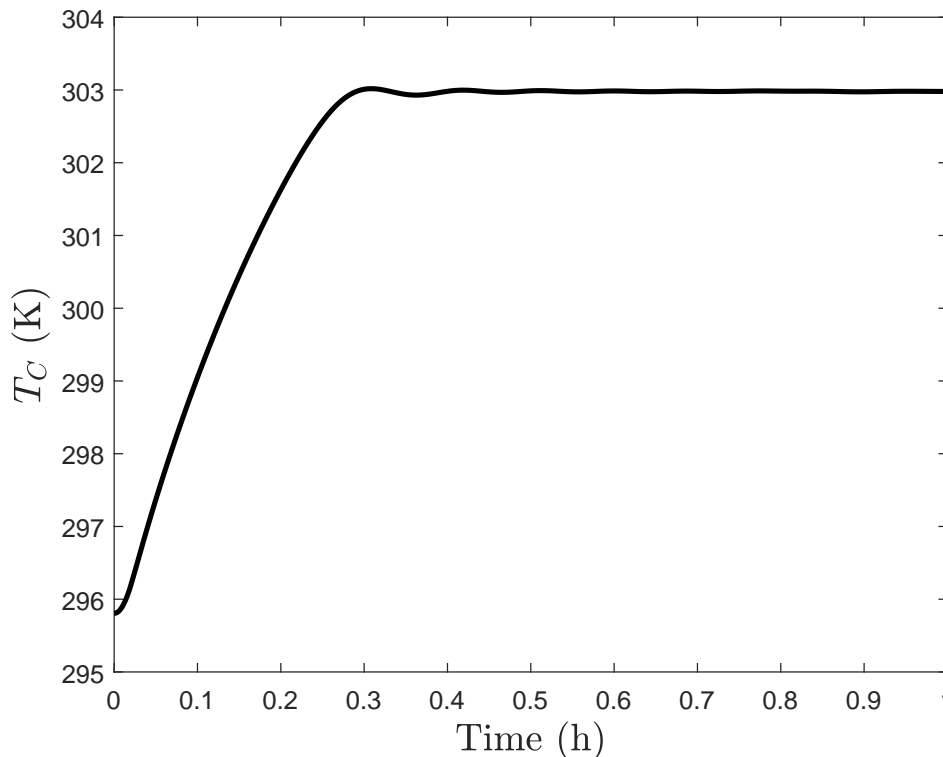
Figure 7: Cold side temperature profile of the heat exchanger at the z = 0 position over time using $v_C = 10$ m/h and with the same inputs from EMPC as used to generate Fig. 3.

Because the flow is counter-current, these effects combine to create the temperature profile shown in Fig. 7. As expected, a more significant difference in temperature on the cold side compared to the initial steady-state value (about 7 K) than that which was previously observed in the bottom plot of Fig. 6 compared to the initial steady-state in that figure is noted due to the smaller cooling fluid flow rate, which requires more heat to be absorbed by the material on the cold side for the same temperature increase on the hot side.

The above results suggest that the process design itself might be used to attempt to lower computation time of the EMPC; specifically, consider a conceptual example in which to meet plant operating objectives, the temperature leaving the cold side of the heat exchanger should be no more than 2 K above the steady-state temperature in that heat exchanger if the CSTR is operated at steady-state (the initial steady-state value is 277.8 K and 295.8 K at z = 0 for the cases where v_C = 50 m/h and v_C = 10 m/h, respectively, as depicted in Fig. 6 and Fig. 7). According to Fig. 6, the heat exchanger with v_C = 50 m/h can satisfy this requirement under the EMPC used to obtain

21

the temperature profile in Fig. 3; in contrast, from Fig. 7 when $v_C = 10$ m/h, the 2 K requirement is violated if that EMPC is implemented. Additional constraints would be required for the EMPC in Fig. 7 to keep the temperature on the cold side within 2 K of its initial steady-state value. To demonstrate the effect of this, we add a hard constraint on the heat exchanger cold side temperature in the EMPC formulation described above (Eq. 6d) that allows a maximum change of 2 K from its steady-state operation value (Fig. 5; i.e., $293.8 \leq T_C \leq 297.8$ K) for the process design with $v_C = 10$ m/h. The heat exchanger model developed using the discretization of the spatial derivatives of T_H and T_C from Eqs. 13-14 was also included in the EMPC formulation (Eq. 6b) to enable the controller to be aware of the dynamics of the CSTR and heat exchanger (which adds arithmetic operations to each evaluation of the constraints of the optimization problem). The simulations were initialized from the steady-state of the CSTR-heat exchanger system with $C_A = C_{As}$, $T = T_s$ and the heat exchanger initial temperature profile in the bottom plot of Fig. 5. The hard constraint on the heat exchanger cold side temperature was enforced at every integration step. The initial guesses for the decision variables were at the upper bounds of C_{A0} for that input, and 10^7 times greater than the upper bound for Q for that input, at each sampling time, unless fmincon did not identify a local minimum after the problem solved once at a sampling time, in which case the optimization problem was re-solved with the solution obtained from the first attempt as the initial guess. Centered finite differences were used for gradient estimation by fmincon.

The heat exchanger hot and cold side temperature profiles at the z = 0 position over one hour of operation using $v_C = 10$ m/h and with control actions computed by this EMPC are delineated in Fig. 8. The variations in T_H over time toward the beginning of the time of operation in Fig. 8 (in the top plot) reflect the manner in which the EMPC operates the process to optimize profit while ensuring the process state constraints are met. In the bottom plot, the somewhat delayed oscillatory response in the heat exchanger cold side temperature profile is due to the combined design factors of cooling fluid selection and cooling fluid flow rate. The maximum and minimum temperatures of the cold side of the heat exchanger at the z = 0 reached over one hour of operation were $T_C = 296.6$ K and $T_C = 295.6$ K, respectively. While the temperature requirement on the cold side of the heat exchanger was respected, the time-averaged production rate of B in the reactor under this

EMPC with the hard constraint on the heat exchanger cold side temperature was 29.0 kmol/h·m^3, which is lower than the 33.2 kmol/h·m^3 achieved in the previous case with no additional constraint. Although it was not checked whether either profit value is a global optimum, this result indicates the general concept that if certain process designs would require additional constraints to be added to an EMPC to ensure that design requirements are met, such designs may reduce the feasible region of operation for the EMPC and thus may potentially lower economic performance from the controller compared to the case that no constraints are required. This indicates that the selection of the process design may determine how flexibly the EMPC can operate the process, which impacts the achievable economic performance of the plant. Furthermore, the need to include the discretized dynamic model of the heat exchanger, requiring the integration of many more states than in the case that this model is not included, in order to enforce the required constraint can increase controller computation time. This section demonstrates that because the EMPC may operate a process at the boundaries of the process constraints to optimize profits, either the EMPC must include all process constraints (which can add complexity to the controller) or the design must ensure that if those constraints are not included, hard process design requirements could be met even with the potential for the controller to operate the process at the limits of the feasible set. This is a manner in which process design and EMPC interact, and which may indicate a potential benefit of simultaneous process and EMPC design even in the absence of disturbances. However, it would only be expected to have significant benefits if the time that it takes to compute the solution for the EMPC was significantly long compared to the timescale on which the states evolve. The example above is meant to be illustrative of the computational complexity concept, but no computation times are reported given that it is a small-scale example and no attempt was made to optimize the codes for speed.

Remark 4. *The type of EMPC implemented in the process was the Lyapunov-based EMPC described by Eqs. 6 and 8. However, the result that the process design may impact EMPC design (by, for example, requiring additional constraints to be added in the controller to ensure that design requirements are met for certain designs and potentially thereby reducing profit under EMPC or changing computation time) is a general conclusion tied to the foundations of optimization-based*
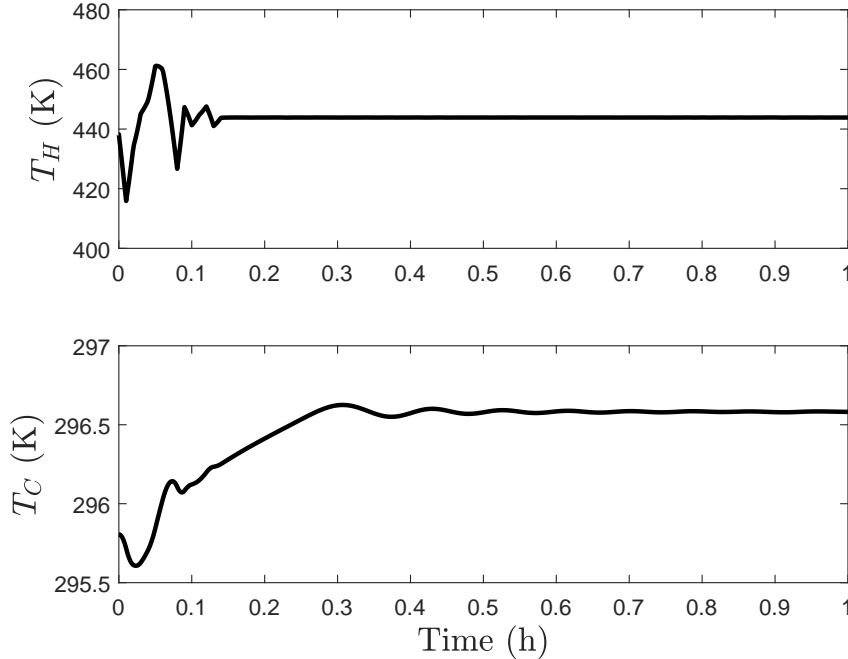
Figure 8: Hot side temperature profile (top plot) and cold side temperature profile (bottom plot) of the heat exchanger at z = 0 position over time using $v_C = 10$ m/h and with inputs from EMPC with the hard constraint on the cold side temperature applied to the CSTR.

control and process design, and is therefore not restricted to a certain EMPC formulation. Conceptually, EMPC formulations share the same structure presented in Eq. 6 but differ from one another in the way constraints are defined and enforced throughout the time of operation. In this example, the process state was driven towards the boundary of the stability region and remained there in Fig. 6. Lyapunov-based stability constraints (Eq. 8) are beneficial in this case as they provide a clear region within which the closed-loop state must stay (though in Fig. 6, the behavior of the process under the EMPC suggests that greater profits are made with respect to Eq. 6a at a different steady-state further from the steady-state (C_{As}, T_s) around which the stability region was designed (i.e., the steady-state around which the stability region was designed is not the economically-optimal steady-state in the above example)).

3.1.1.2. CSTR and Heat Exchanger Analysis B: Sequential Versus Simultaneous Design Frameworks. The above example suggests that designing a process and an EMPC at the same time might be beneficial in the case that a decentralized control design is being used. Specifically, the above section suggests that one way of reducing computational complexity of the control design may be

to attempt to take advantage of the design itself to reduce the need to make the controller aware of process constraints or of the models of other parts of the process. Then, the controller can include another constraint (to be referred to as a "pseudo" constraint below since it is not fully representative of the quantity which it is desired to constrain) which can be tuned to ensure that the desired process constraint is met. This section demonstrates this concept by showing how this might be done for the above example, and then compares the concept with sequentially designing the process and controller (i.e., designing the controller before the process, and finding an optimal process design in light of the control strategy) in the absence of disturbances.

To demonstrate how a simultaneous process/EMPC design approach may be undertaken to reduce EMPC computational complexity using a "pseudo" constraint, we consider the same system of a CSTR followed by a counter-current heat exchanger presented in Section 3.1.1.1 but in which the cooling fluid heat capacity (C_{pC}) is 0.8 kJ/kg·K. For the CSTR under consideration, we consider that the goal of the simultaneous process design and control approach is to select process and controller design parameters to maximize the revenue minus capital costs while meeting operating requirements (defined as a need to keep the outlet temperature of the cold side of the heat exchanger no more than 2 K above its initial temperature for a given value of v_C if the CSTR is operated at the steady-state $C_{As} = 1.22$ kmol/m^3, $T_s = 438.2$ K, $C_{A0s} = 4$ kmol/m^3, and $Q_s = 0$ kJ/h).

To determine decision variables and constraints to use in a simultaneous EMPC and process design framework, we note that it is expected that changes in the value of v_C could impact the capital cost of the system as well as the process design constraint, and therefore the process decision variable p_{dv} in the simultaneous process and EMPC design approach was selected to be v_C. Specifically, the process design constraint is that the difference between the maximum temperature achieved on the cold side of the heat exchanger ($T_{C,max}$, corresponding to T_C when z=0) and the initial steady-state value at z=0 (T_{Cs}) must be below a heat exchanger cold side temperature requirement (where the values of the steady-state temperature at the z=0 position on the hot and cold sides of the heat exchanger, denoted by T_{Hs} and T_{Cs}, respectively, change based on the value of v_C). We defined this operating requirement to be $T_{Cs} - 2 \leq T_{C,max} \leq T_{Cs} + 2$. For this requirement, higher values of v_c would prevent the temperature of the cold side of the heat exchanger from varying as much down

its length for larger values of the temperature of the stream at the heat exchanger inlet. Here, we consider the cold side fluid flow rate to be a design decision in the sense that we are seeking to design a process that has that fluid flow rate (i.e., it is not available to be manipulated by EMPC to take any value in its bounds to optimize profit, but the process is being designed to keep that fluid flow rate at its design value; if the cold side fluid flow rate was used as a decision variable by the EMPC, then another process design decision variable would need to be selected to analyze process and EMPC design interactions, but this is not done here for simplicity).

To make the EMPC fully aware of the constraint on the temperature on the cold side of the heat exchanger would require that the heat exchanger model of Eqs. 13-14 be solved within the EMPC. This introduces a number of states to represent the discretized form of these equations, which would need to be numerically integrated with an integration step smaller than that of the CSTR alone if the Explicit Euler numerical integration method is used. Though other numerical methods could be used to work with this system as well, we explore the concept of eliminating the need to account for the heat exchanger solution in the EMPC by instead placing a bound on the temperature of the fluid entering the heat exchanger on the hot side. This can be represented as a bound on the temperature of the fluid in the CSTR and therefore is able to be placed within the EMPC without the simulation of the heat exchanger explicitly within the controller. Because the value of Eq. 15 (representative of revenue over the prediction horizon) increases as the temperature at the CSTR outlet increases (reflected in Fig. 6), but it also increases the outlet temperature of the cold side of the heat exchanger (thereby impacting how close the operating requirements on the cold side outlet temperature described above come to being violated), it was anticipated that the simultaneous process and EMPC design for this example should contain a decision variable reflecting the upper bound on the temperature in the CSTR that is used by the EMPC (T_{ub}, which was allowed to be selected within the range $470 \leqslant T_{ub} \leqslant 500$ K; this constraint acts as the "pseudo" constraint since it is not a direct bound on the 2 K operating requirement, but through tuning via the simultaneous process and EMPC design approach, may be able to ensure that that requirement is met). Therefore, $c_{dv} = T_{ub}$.

To develop the objective function of Eq. 9, both the capital cost term $Cost$ and the instantaneous

revenue R_e must be defined for this example. We will analyze a case in which the capital cost in Eq. 9a is formulated as follows:

$$Cost = 0.00671((31.1329 v_C A_C - 600.87)^2 + (31.1329 v_C A_C - 600.87)) + 201.34 \qquad (17)$$

This equation was selected to cause the capital cost ($Cost$) in Eq. 9a to have a parabolic behavior and be on the same order of magnitude as the revenue in the 0.5 h of operation. This cost function was numerically selected for the purposes of analyzing the proposed framework. R_e in Eq. 9a was set to be L_e in Eq. 15, but scaled by a factor of 27.56 assumed to convert the value of L_e to currency units (\$) such that both terms in the global economic cost function of Eq. 9a have the same units. The prediction horizon and sampling period in Eq. 10 were set to $N = 2$ and $\Delta = 0.01$ h, respectively.

The explicit Euler numerical integration method was applied to simulate the CSTR in Eqs. 11-12 with an integration step of 10^{-4} h in both Eqs. 9 and 10. The method of lines described in Section 3.1.1 with 19 interior nodes and 2 boundary nodes for the spatial integration, with the Explicit Euler numerical integration method using an integration step of 10^{-6} h, was implemented to make predictions for the heat exchanger states in Eq. 9. The piecewise constant input trajectory is obtained from Eq. 10 and applied to Eq. 9 to evaluate the global objective function under a given combination of design decision variables. No Lyapunov-based stability constraints were applied. Conceptually, the formulation of Eqs. 9-10 for this example is as follows:

$$\min_{v_C, T_{ub}} \quad Cost - 27.56 \int_0^{t_f = 0.5h} [k_0 e^{-\frac{E}{R\hat{T}(\tau)}} \hat{C}_A(\tau)^2] \, d\tau \qquad (18a)$$

$$\text{s.t.} \quad [C_{A0}(t) \ Q(t)]^T = [C_{A0}^*(t_k|t_k) \ Q^*(t_k|t_k)]^T, k = 0, \ldots, (t_f/\Delta - 1), \forall t \in [t_k, t_{k+1}) \qquad (18b)$$

$$\frac{d\hat{C}_A}{dt} = \frac{F}{V}(C_{A0} - \hat{C}_A) - k_0 e^{-\frac{E}{R_g \hat{T}}} \hat{C}_A^2 \qquad (18c)$$

$$\frac{d\hat{T}}{dt} = \frac{F}{V}(T_0 - \hat{T}) - \frac{\Delta H k_0}{\rho_L C_p} e^{-\frac{E}{R_g \hat{T}}} \hat{C}_A^2 + \frac{Q}{\rho_L C_p V} \qquad (18d)$$

$$\frac{\partial \hat{T}_H}{\partial t} = -v_H \frac{\partial \hat{T}_H}{\partial z} + \frac{h A_s}{\rho_L A_H C_p}(\hat{T}_C - \hat{T}_H) \qquad (18e)$$

$$\frac{\partial \hat{T}_C}{\partial t} = v_C \frac{\partial \hat{T}_C}{\partial z} + \frac{h A_s}{\rho_C A_C C_{pC}}(\hat{T}_H - \hat{T}_C) \qquad (18f)$$

$$\hat{C}_A(t_0 = 0) = C_{As} \qquad (18g)$$

$$\hat{T}(t_0 = 0) = T_s \tag{18h}$$

$$\hat{T}_H(z, t_0 = 0) = T_{Hs}(z) \tag{18i}$$

$$\hat{T}_C(z, t_0 = 0) = T_{Cs}(z) \tag{18j}$$

$$T_{Cs} - 2 \leq T_{C,max} \leq T_{Cs} + 2 \tag{18k}$$

$$470 \text{ K} \leq T_{ub} \leq 500 \text{ K} \tag{18l}$$

$$180 \text{ m/h} \leq v_C \leq 220 \text{ m/h} \tag{18m}$$

$$\begin{bmatrix} C_{A0}^*(t_k|t_k) \\ Q^*(t_k|t_k) \end{bmatrix} = \text{ones}(m, m(N-1)) \begin{bmatrix} \hat{C}_{A0}(t_k) \\ \hat{Q}(t_k) \end{bmatrix} \tag{18n}$$

$$[\hat{C}_{A0}(t_k) \ \hat{Q}(t_k)] = \underset{\bar{C}_{A0}(t), \bar{Q}(t) \in S(\Delta)}{\arg\min} \quad -\int_{t_k}^{t_{k+N}} [k_0 e^{-\frac{E}{R\tilde{T}(\tau)}} \tilde{C}_A(\tau)^2] \, d\tau \tag{19a}$$

$$\text{s.t.} \quad \frac{d\tilde{C}_A}{dt} = \frac{F}{V}(\bar{C}_{A0} - \tilde{C}_A) - k_0 e^{-\frac{E}{R_g\tilde{T}}} \tilde{C}_A^{\ 2} \tag{19b}$$

$$\frac{d\tilde{T}}{dt} = \frac{F}{V}(T_0 - \tilde{T}) - \frac{\Delta H k_0}{\rho_L C_p} e^{-\frac{E}{R_g\tilde{T}}} \tilde{C}_A^{\ 2} + \frac{\bar{Q}}{\rho_L C_p V} \tag{19c}$$

$$\tilde{C}_A(t_k) = \hat{C}_A(t_k) \tag{19d}$$

$$\tilde{T}(t_k) = \hat{T}(t_k) \tag{19e}$$

$$\tilde{T}(t) \leq T_{ub}, \ \forall \ t \in [t_k, t_{k+N}) \tag{19f}$$

$$0.5 \text{ kmol/m}^3 \leq \bar{C}_{A0} \leq 7.5 \text{ kmol/m}^3 \tag{19g}$$

$$-5.0 \times 10^5 \text{ kJ/h} \leq \bar{Q} \leq 5.0 \times 10^5 \text{ kJ/h} \tag{19h}$$

The constraint of Eq. 19f is enforced at every integration step. In Eqs. 18i and 18j, $\hat{T}_H(z, t_0) = T_{Hs}(z)$ and $\hat{T}_C(z, t_0) = T_{Cs}(z)$ represent that the initial values of the hot and cold side temperature profiles, respectively, at z = 0 are set to the steady-state values which correspond to the hot side inlet taking the value of T_s, and the cold-side outlet temperature then being set by solving for the steady-state of Eqs. 13-14 with T_C at z = L set to 273 K, and with the value of v_C being tested as a possible optimal solution to Eq. 18.

To obtain insights into the interactions between process and EMPC design but with reasonable computational complexity, we do not attempt to rigorously solve the simultaneous design and control algorithm in Eqs. 18-19, but instead attempt to gain insights into factors that are expected to play

a role in the formulation and effectiveness of that methodology by discretizing the allowable range of values of the decision variables using unitary increments for T_{ub} and v_C, and assessing the global cost function for those combinations of T_{ub} and v_C. Specifically, we discretize the two decision variables, v_C and T_{ub}, in increments of 1 over their allowable ranges (between 470 K and 500 K for T_{ub} and 180 m/h and 220 m/h for v_C). For each resulting v_C-T_{ub} combination, we evaluated the global cost function (Eq. 18a) when EMPC was implemented in each process system designed with the combination of decision variables, and t_f was set to 0.5 h with C_A and T initialized from C_{As} and T_s. fmincon was utilized to solve the EMPC for each T_{ub} and v_C combination explored on a desktop Intel(R) Xeon(R) CPU E-3 1240 v5 at 3.50GHz, with a 64-bit operating system with an x64-based processor running Windows 10 Enterprise, in MATLAB R2016a. In the optimization problem, the value of Q was scaled down by 10^7 to address its larger order of magnitude compared to the other terms in the process model, and the initial guess for the control actions from the EMPC was the steady-state value of the inputs at each sampling time, unless fmincon identified a potential local minimum, in which case the optimization problem was re-solved with the solution obtained from the first attempt as the initial guess. Notably, no attempt was made to make the control actions computed by fmincon global solutions at any sampling time for any combination of decision variables of Eq. 18. To prevent high computation times, short prediction horizons ($N = 2$) were used. Though this implementation may not find the global optimal solution and the time of operation considered is much shorter than a plant's life, these simplifications allowed insights into design-control interactions under EMPC to be obtained with reduced computation time.

The best values of the decision variables among those tested via the approach used for analyzing characteristics of the feasible solution space for this example with $N = 2$ (i.e., checking for the best values of T_{ub} and v_C among values within the discretized ranges of these variables as described above), over 0.5 h of operation using MATLAB, were T_{ub} =490 K and v_C =195 m/h. The trajectories of the states and inputs of the CSTR under the EMPC with these values of the design parameters are depicted in Figs. 9-10, with the process states initialized from their initial steady-state values. As shown in Fig. 9, the outlet temperature of the CSTR reaches approximately 490 K and then it remains at this value to maximize the process profit. The hot and cold side temperature profiles at
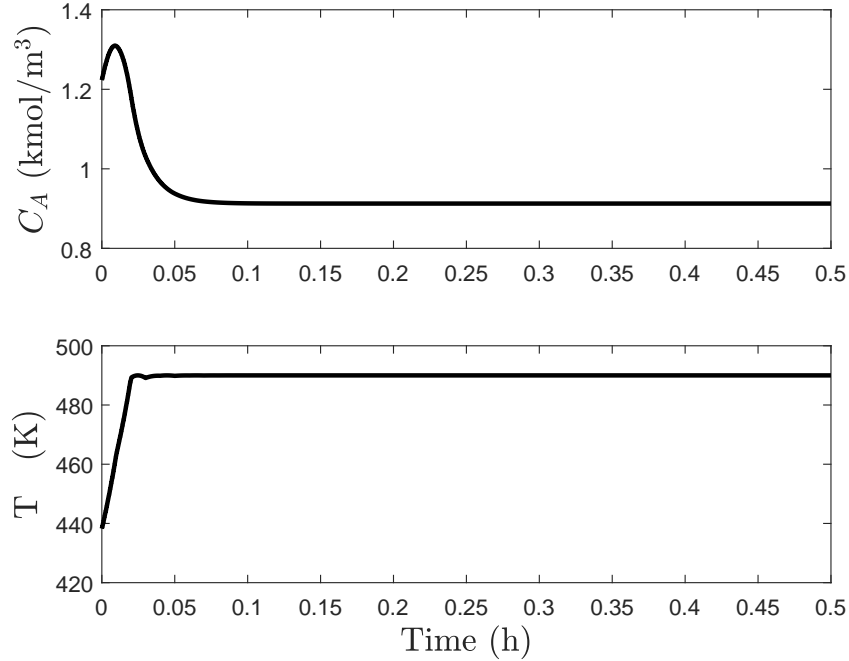
Figure 9: States over 0.5 h of operation for the process of Eqs. 11-12 under the EMPC designed using the simultaneous process and EMPC design approach with the global objective function based on Eq. 17.

the z = 0 position of the heat exchanger over time are presented in Fig. 11. We can observe that the design constraint was met as the initial heat exchanger cold side temperature was 279.37 K and the maximum temperature achieved on the cold side was 281.36 K (i.e., a 1.99 K difference from the initial steady-state value, which is below the heat exchanger cold side temperature requirement). These results indicate that the best feasible solution among those tested for the EMPC-process design combination coming from the simultaneous process and EMPC design approach allowed the design constraints to be met with only the T_{ub} constraint in the EMPC, while maximizing the profit.

The values of v_C and T_{ub} that gave the largest value for the global objective function among those tested are not at the bounds of either decision variable. Though this problem was not solved to global optimality so that this $v_C - T_{ub}$ combination is not necessarily globally optimal, it highlights the concept that the greatest utility of the simultaneous process and EMPC design approach would be expected to be in cases where a trade-off exists that causes the optimal values of the decision variables to not easily be known *a priori*. The objective function of Eq. 17 was designed to potentially have such a trade-off because according to Eq. 17, the capital cost term
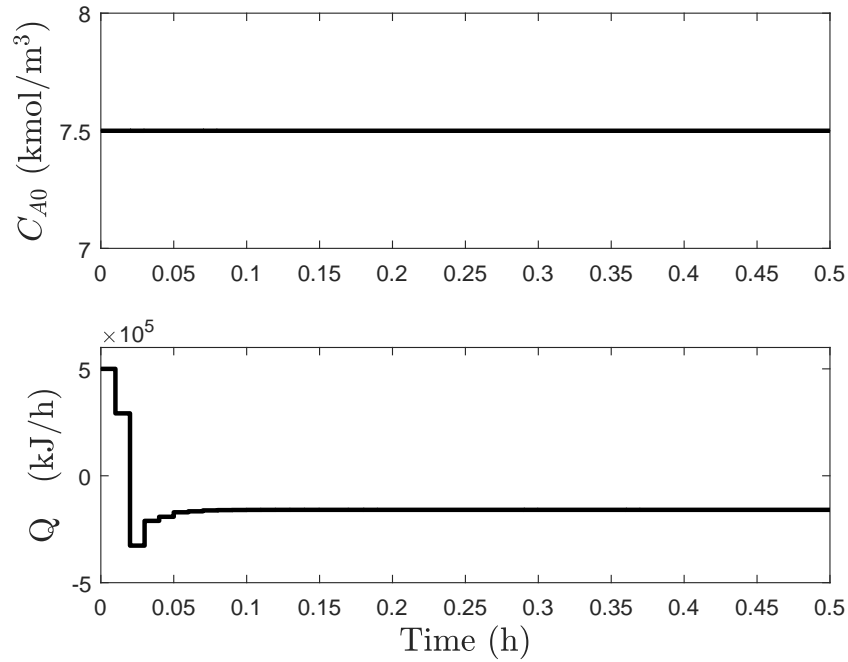
Figure 10: Inputs over 0.5 h of operation for the process of Eqs. 11-12 under the EMPC designed using the simultaneous process and EMPC design approach with the global objective function based on Eq. 17.
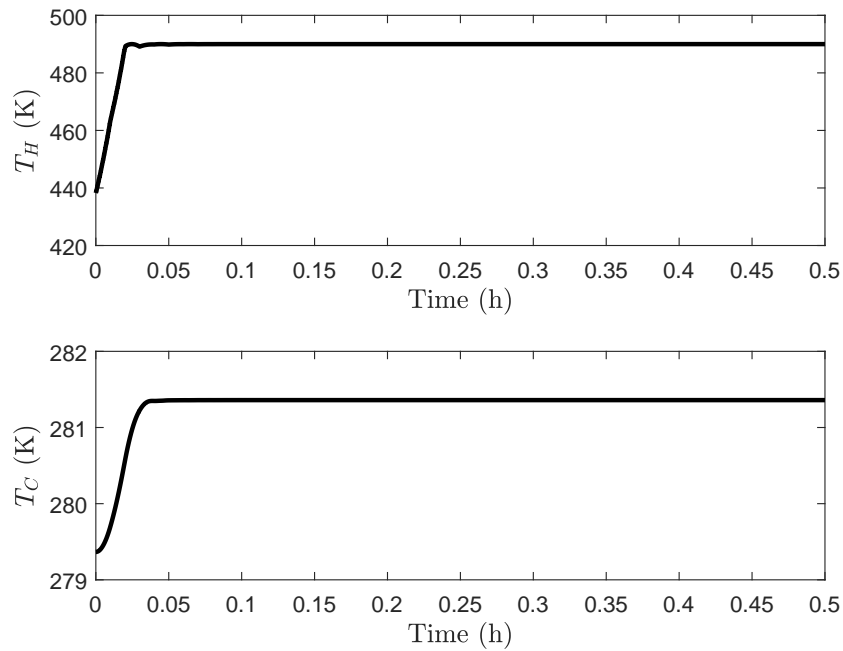
Figure 11: Hot and cold side temperature profiles of the heat exchanger at the $z = 0$ position over time and with control actions for the CSTR from EMPC designed using the simultaneous process and EMPC design approach with the global objective function based on Eq. 17.

has a parabolic behavior (it has the minimum cost value around $v_C = 193$ m/h), but the revenue term relies on both v_C (which sets the steady-state hot and cold side temperature profiles in the heat exchanger) and T_{ub} (as v_C increases, the temperature at which the CSTR can be operated increases and, consequently, the production rate of species B becomes greater) and can potentially be increased more than the capital cost term as v_C rises.

However, a simultaneous design framework is not guaranteed to give values of the design parameters that are not intuitive/not at the bounds of the design parameters. For example, we can explore the simultaneous design and control problem with an alternative objective function as follows:

$$Cost = 5.71 \times 10^{-5} exp(12.1656 + 0.0862[ln(31.11 v_C A_C)]^2) \tag{20}$$

This equation is a modified correlation of a pump purchase cost equation from Seider et al. (2017), where the modifications were selected to cause the capital cost ($Cost$) in Eq. 18a to be close to the same order of magnitude as the revenue in the 0.5 h of operation. With this objective function, with the discretization of the decision variables T_{ub} and v_C using unitary increments within their bounds and after performing a simulation for 0.5 h of operation for each T_{ub} and v_C pair, the resulting best combination of decision variables among the feasible solutions tested was $v_C = 180$ m/h and $T_{ub} = 486$ K, using MATLAB R2016a on a desktop Intel(R) Xeon(R) CPU E-3 1240 v5. For the process simulated with this $v_C - T_{ub}$ combination (in MATLAB R2017b on an Intel(R) Core(TM) i7-7500U CPU at 2.70GHz, 2.90GHz, with 16.0 GB of memory and a 64-bit operating system with an x64-based processor running Windows 10 Enterprise), the design constraint was met as the initial heat exchanger cold side temperature was 279.89 K and the maximum temperature achieved on the cold side was 281.88 K. In this case, v_C is at its lower bound partially due to the objective function formulation and the manner in which it depends on v_C. Due to the EMPC design, for a given v_C, T_{ub} should be the highest value possible that will cause all the process predictions over the time of operation to be within the allowable region in which the heat exchanger cold side temperature requirement is respected. Though again global optimality was not searched for, the same set of potential $v_C - T_{ub}$ combinations were tested with Eq. 17 as with Eq. 20, and the difference in which of these was optimal for a given objective function highlights that different objective functions can

give different optimal solutions and that with some objective functions, the best design decision may be evident from process knowledge without using a simultaneous design and control approach. Both in testing multiple values of $v_c - T_{ub}$ and simulating the process with the best among those tested, Q was scaled down by 10^7, and the initial guess for the control actions from the EMPC was the steady-state value of the inputs at each sampling time, unless fmincon did not identify a local minimum after the problem solved once at a sampling time so that then the optimization problem was re-solved with the solution obtained from the first attempt as the initial guess.

Though the results above indicate that there may be some benefit in some circumstances to seeking to find the solution to a simultaneous design and control problem even in the absence of disturbances in the case that a decentralized EMPC is desired to be designed (here, for example, a constraint in the controller is being designed not with respect to hard bounds on process physics or safety objectives, but as a surrogate meant to represent some other hard process constraint approximately in the control design to reduce the controller computation time), the formulation of EMPC offers great power for including all process knowledge. Specifically, like steady-state tracking MPC, it can account for process constraints explicitly in the control design, but unlike tracking MPC, it is also fully aware of a description of the process economics (MPC is aware of an objective function that can be tuned to be the best representation of the process economics possible, but is not fundamentally representative of the process economics in many cases). This fact means that, whereas traditional steady-state tracking control designs must be developed after a process design is determined (because they contain parameters that have to be tuned to achieve the best economics for a given process design) or at best be determined at the same time as the process parameters, centralized EMPC, in the absence of disturbances, is best designed to be as flexible as possible (but with constraints imposed by physical or safety limitations) before the process and then used to guide the process design by simulating various process designs under the EMPC aware of the various process models as they are updated to see which process dynamics provide the EMPC the greatest flexibility to optimize economics within the constraints. This also means that a primary benefit of considering EMPC in a sequential design and control framework in the absence of disturbances is that it offers an automated framework for removing a steady-state mentality from

design considerations, but still allows the possibility that the design found is one which corresponds to the controller driving the closed-loop state to a steady-state. This indicates that whereas process design has traditionally come before control design, we here suggest control design before process design in the absence of disturbances due to the special character of EMPC.

Remark 5. *Because the focus of this work is on elucidating the relationships between process and EMPC design in the absence of disturbances, rather than on developing novel algorithms for solving that problem efficiently, computation time reduction techniques would be needed to be investigated for cases where the simultaneous design of process and control is advantageous. Given our focus, no attempt was made to use an efficient optimization method/software or to optimize the codes in this work. Even the method used in determining values of v_C and T_{ub} that would be most profitable in a simultaneous design and control framework did not solve the bilevel optimization problem, but instead discretized (in a relatively coarse fashion) the decision variables to evaluate the objective function at a number of v_C-T_{ub} combinations, which we recognize is not an efficient method to solve this problem.*

Remark 6. *Though a short prediction horizon of $N = 2$ was used in the simultaneous design and control framework, the state and input trajectories under EMPC when T_{ub} is 490 K with $N = 2$ and $N = 5$ and with the EMPC formulated according to Eq. 19 were almost overlaid. In cases where the input trajectories under the control laws which are available to be selected while searching for a simultaneous design and control strategy are similar with different prediction horizons, it is possible that changing the prediction horizon may not change the optimal design.*

Remark 7. *In this example, no lower bound was imposed on the temperature in the CSTR in the EMPC because it was known that the EMPC would increase temperature above the initial value in order to maximize the objective function of Eq. 15.*

Remark 8. *Other process design variables besides v_C (e.g., reactor volume or heat exchanger area) could have been examined. These changes would be expected to impact profits and could lead to optimal designs with different design parameters than were used in the simulations in this work. As design parameters are changed, they can impact the steady-state for the CSTR to operate around; for*

LEMPC, this could require a new stability region, Lyapunov function, and Lyapunov-based controller to be designed each time the design parameters are adjusted. For other EMPC formulations, another aspect of the controller might need to be adjusted (e.g., the terminal steady-state condition would need to be updated for a terminal equality constraint EMPC).

3.1.1.3. CSTR and Heat Exchanger Analysis C: Controller Computational Complexity for Other EMPC Formulations via Simultaneous Process/Control Design. In the above sections, the simultaneous design and control framework was analyzed for a transient that lasts for a very small fraction of the time of plant operation in the absence of disturbances. Therefore, though the above sections demonstrated that there may be potential for benefits for a simultaneous process and EMPC design framework for computation time reduction of the EMPC if a process operates in a transient fashion for a short period of time, it did not provide an example that indicated that similar conclusions might hold when the transients last longer.

To force the process in Section 3.1.1.1 (i.e., C_{pC} is again 4.18 kJ/kg·K) to operate in a transient fashion for a longer period of time to examine this case, we can consider a limit on the time-averaged amount of reactant fed to the reactor in one hour of operation. Eq. 21 reflects this economics-oriented constraint, which we will seek to approximately satisfy:

$$\frac{1}{1 \text{ h}} \int_{t=0 \text{ h}}^{t=1 \text{ h}} u_1(\tau) d\tau = 0 \text{ kmol/m}^3 \tag{21}$$

Since the EMPC using the process model of Eqs. 11-12, the Lyapunov-based stability constraints of Eqs. 8a-8b, and the bounds on the inputs ($0.5 \leq C_{A0} \leq 7.5$ kmol/m^3 and $-5.0 \times 10^5 \leq Q \leq 5.0 \times 10^5$ kJ/h) is not guaranteed to be feasible with Eq. 21, the constraint of Eq. 21 was implemented using slack variables, s_1 and s_2, as in Durand (2019):

$$s_1 \geq \sum_{i=0}^{k-1} (u_1^*(t_i|t_i)) + \sum_{i=k}^{k+N_k} (u_1(t_i|t_k)) - 3.5\delta(100 - \frac{t_k}{\Delta} - N) \tag{22}$$

$$s_2 \geq -\sum_{i=0}^{k-1} (u_1^*(t_i|t_i)) - \sum_{i=k}^{k+N_k} (u_1(t_i|t_k)) - 3.5\delta(100 - \frac{t_k}{\Delta} - N) \tag{23}$$

where $N_k = N$ and $\delta = 1$ for $t_k < 0.9$ h, and $\delta = 0$ and N_k is set to the number of sampling periods remaining in the operating period of one hour when $t_k \geq 0.9$ h. The upper and lower bounds of s_1

and s_2 were 2×10^{19} and -2×10^{19}, respectively, and the initial guess for these decision variables provided to fmincon was 0 at each sampling time. The objective function of the EMPC to be minimized with the slack variables is presented below:

$$\int_{t_k}^{t_{k+N}} \left[-k_0 e^{-\frac{E}{R_g T(\tau)}} C_A(\tau)^2 \right] d\tau + 100(s_1^2 + s_2^2) \tag{24}$$

The weight coefficient of 100 given to the slack variable term was chosen to attempt to drive the slack variables toward zero to prevent violations of the material constraint of Eq. 21 while avoiding significant reduction of the profit defined by the objective function of Eq. 24. Simulations of the process of Eqs. 11-13 with $v_C = 50$ m/h were performed, initialized from $C_A = C_{As}$, $T = T_s$, and the heat exchanger initial temperature profile in Fig. 5 (top plot), for 10 h of operation. The hot and cold side temperature profiles of the heat exchanger at the z = 0 position over 10 h of operation under this EMPC are depicted in Fig. 12. These plots were generated in MATLAB R2016b on a Lenovo model 80XN x64-based ideapad 320 using fmincon with Q scaled down by 10^7, the centered finite difference method utilized by fmincon, and the initial guess of the decision variables being their steady-state unless a local minimum was not located, in which case the solution that was not a local minimum became the initial guess.

The time-averaged amount of material fed to the reactor in each hour of operation was 0.4 kmol/m^3, slightly above the desired value of 0 kmol/m^3 from Eq. 21. It can be seen in Fig. 12 that the temperature on the hot side of the heat exchanger reaches its maximum at 491.7 K and remains again around 490 K for about 0.4 h in each operating period to maximize the reaction rate in the CSTR. After this, the temperature drops to a minimum around 406 K, remains there for about 0.4 h and then increases to reduce the violation of the material restriction imposed by Eq. 21.

In terms of the impact of this material constraint on the process design procedure without disturbances, we note that the heat exchanger cold side temperature profile follows a behavior qualitatively similar to the hot side temperature profile, but the temperature change is less than 2 K from its initial value at the z = 0 position (277.8 K), as observed in Fig. 12. Despite the variation in T_H over time, the temperature variation on the cold side of the heat exchanger was relatively small for this cooling fluid flow rate. If instead the temperature profile in the top plot of Fig. 12 is
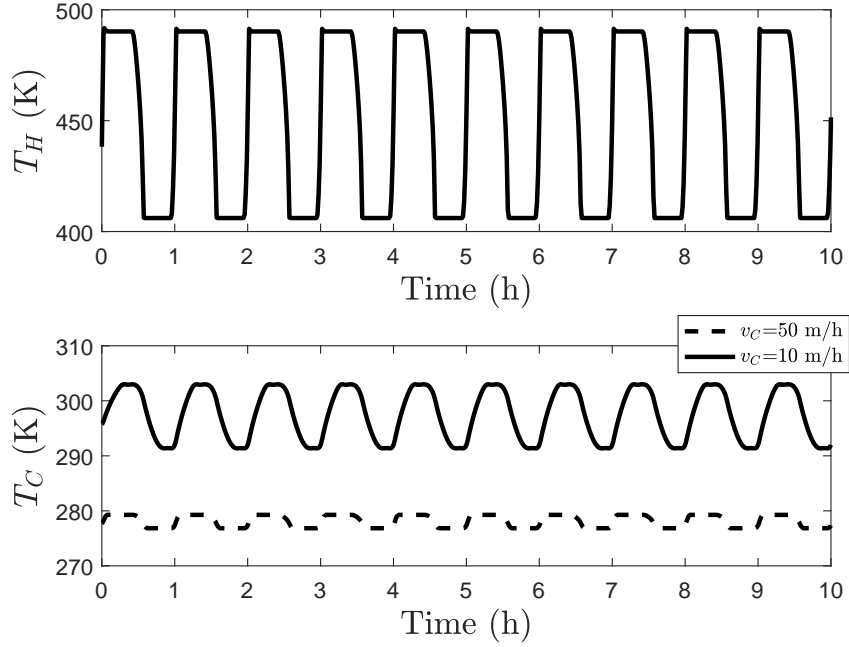
Figure 12: Hot side temperature profile of the heat exchanger at the z = 0 position over time and with inputs from EMPC with the material constraint applied to the CSTR (top plot) and cold side temperature profile of the heat exchanger at the z = 0 position over time using $v_C = 50$ m/h and with $v_C = 10$ m/h with inputs from EMPC with the material constraint applied to the CSTR (bottom plot).

used as the hot side inlet temperature for the heat exchanger when $v_C = 10$ m/h (initialized from the steady-state temperature profile in the bottom plot of Fig. 5), the cold side temperature profile at the z = 0 position over one hour of operation is shown in Fig. 12 (in the bottom plot). The heat exchanger cold side temperature profile shows a temperature change of more than 2 K from its initial value at the z = 0 position (295.8 K), as shown in Fig. 12. As for Figs. 6 and 7, we again conclude that even with this different operating policy computed by the EMPC (Fig. 6 compared to Fig. 12), the process design may impact the constraints required in the EMPC. These results indicate that both for $v_c = 50$ m/h and $v_c = 10$ m/h, the temperature on the hot side of the heat exchanger is brought to an upper bound for a period of time under the material constraint (due to the objective function being maximized at a point in the stability region with a temperature higher than that at the initial condition), but then as the constraint changes over time, it eventually forces the closed-loop state to leave that optimal operating point. Here, then, the value of T_{ub} would still need to be designed for the worst-case steady-state that the process sees over time (i.e., the value of

T_{ub} should be that which ensures that the temperature of the cold fluid leaving the heat exchanger at a steady-state temperature coming in to the hot side of the heat exchanger is not greater than the 2 K requirement). This implies that time-varying operation may not necessarily result in a different set of design parameters than if the closed-loop state was driven to a steady-state value in the stability region.

3.1.1.4. CSTR and Heat Exchanger Analysis D: EMPC Prediction Horizon and Simultaneous Process/Control Design. Section 3.1.1.2 hinted at the implications of the prediction horizon length for the simultaneous process and EMPC design problem; in this section, we discuss its role more explicitly. First, it may be beneficial to perform a process design selection with an EMPC with a prediction horizon and sampling period which give equivalent input trajectories to those from the EMPC with the prediction horizon and sampling period planned to be utilized, as different prediction horizons and sampling periods may create different profits and even a different character of the trajectories of the states under the computed inputs. Depending on the prediction horizon and dynamics, it may be possible to achieve such trajectories while predicting for a shorter time into the future than is planned in the EMPC to be utilized, such that EMPC's with shorter times of prediction could be utilized in place of those with longer prediction horizons in the simultaneous process and EMPC design framework to reduce computation time of that framework. However, changing the prediction horizon or sampling period from that planned in practice for the simultaneous design problem would need to be done with care.

For example, the prediction horizon can have a significant impact on some designs, for certain EMPC formulations. To see this, consider that a terminal steady-state constraint Rawlings et al. (2012); Mayne et al. (2000) is added to the EMPC in Section 3.1.1.2 to enforce that the heat exchanger hot side temperature at the hot side inlet must be at the initial steady-state value (T_s) at the end of the prediction horizon (i.e., $T(t_{k+N}) = T_s$). Then, with smaller prediction horizons, this constraint maintains the temperature of the CSTR closer to the initial steady-state condition whereas with a larger prediction horizon, the controller has more flexibility to compute control actions that would maximize the profit and meet operating requirements while still meeting the

terminal constraint. The result of this is that an EMPC policy with a larger N would drive the temperature of the CSTR further from the initial steady-state to achieve higher profit, so that with the shorter prediction horizon, the temperature in the EMPC never goes far above its steady-state value.

To see this, we can return to the process in Section 3.1.1.2 (i.e., $C_{pC} = 0.8$ kJ/kg·K), using the simultaneous process and EMPC design procedure as in Eqs. 18-19, with $Cost$ defined by Eq. 17, but where a terminal constraint is added to the EMPC in Eq. 19. Using the same discretization of the v_C and T_{ub} ranges as in Section 3.1.1.2, the most profitable design among those tested when $N = 2$ was $v_c = 193$ m/h with $T_{ub} = 498$ K (though various other designs gave approximately the same profit, indicating that due to the shortness of the prediction horizon combined with the terminal constraint, the control actions did not change much as T_{ub} changed for many values of T_{ub}, so that many values of T_{ub} caused the closed-loop state to give approximately the same profitability when v_c was 193 m/h), whereas when $N = 5$, it was $T_{ub} = 490$ K and $v_c = 195$ m/h (the simulations with $N = 2$ were run in MATLAB R2016a, whereas the simulations with $N = 5$ were run in MATLAB R2018a, on an Intel(R) Xeon(R) CPU E-3 1240 v5, both with Q scaled by 10^7, centered finite differences in fmincon, and initial guesses at the steady-state unless a solution that was not necessarily a local minimum had to be re-used as the initial guess for re-solving the optimization problem). A simulation of the process with the most profitable designs among those tested for each prediction horizon (performed in MATLAB R2016b on a Lenovo model 80XN x64-based ideapad 320 with an Intel(R) Core(TM) i7-7500U CPU) indicated that when $N = 2$, the short prediction horizon caused the maximum temperature reached in the CSTR to be 455.83 K, whereas for $N = 5$, the maximum temperature reached was 490 K. The terminal constraint therefore also restricted the heat exchanger cold side temperature changes when $N = 2$, but with $N = 5$, the same best design decisions ($T_{ub} =$490 K and $v_C =$195 m/h) as the case for EMPC without the terminal constraint were identified due to the fact that this EMPC design had greater freedom to compute inputs to the process that maximize the profit compared to the EMPC formulated using the terminal equality constraint with a smaller prediction horizon. These results highlight that there may be benefit in employing a receding horizon in a simultaneous EMPC and process design framework for some

cases, with the purpose of ensuring that the characteristics of process operation under the expected controller implementation are captured by the simultaneous design and control framework, and also highlight that there is not necessarily a single value of controller design variables which will be optimal for the process.

3.1.2. Study 2: Exploring Conditions for Time-Varying Operation Under EMPC

The results above suggest, though discussed with respect to their potential implications for relationships between time-varying operation and design by evaluating controller behavior in combination with process design over a short timescale, that there may be times that an optimal steady-state analysis may be sufficient for designing an EMPC and process. Specifically, based on Fig. 6, it is expected that after 0.5 h, the profit is dominated by the instantaneous revenue at the final temperature which the CSTR reaches. If there are no disturbances such that the CSTR temperature is then kept at the value that it reaches for all future times by the EMPC, the transient behavior in the first 0.5 h of the simulation would not play a role in the selection of the values of v_C and T_{ub}. Potentially, therefore, if long-term operation had been considered as would be typical in practice (though this example did not consider that to focus on the time-varying aspect of the problem, which was considered to be more informative for elucidating potential interactions between EMPC and process design), this problem could have been explored as a steady-state optimization problem, where the optimal steady-state values of Q and C_{A0} could have been searched for, as well as the optimal value of v_C, to optimize the objective function of Eq. 18a. The value of T reached at this optimal condition (which is the steady-state value of T corresponding to the selected steady-state Q, C_{A0} and v_C) where the design constraint was not violated could then have been considered as T_{ub} in the EMPC formulation. This result implies that for some processes under EMPC, the details of the EMPC formulation may not be required in an optimization-based process/EMPC design procedure. Furthermore, if the capital cost is far less than the revenue over the time of operation, it may be sufficient to select the design variables based on their impact on the controller's ability to optimize revenue only, subject to design constraints.

Though the above section clarifies potential relationships between EMPC and process design in the case where the process transient is noticeable, it begs the question of whether there are expected

to be cases when steady-state operation would not be the optimal operating strategy under EMPC in the absence of disturbances (i.e., it is reasonable to ask whether the relationships between design and EMPC developed in the prior section for a case where the process transients mattered to the conclusions would be meaningful from a long-term process and control design perspective). This section seeks to address this question by again referring to the CSTR from Section 3.1. However, this section will explore the question using EMPC's with different control laws. In the sections below, these EMPC's are used to examine potential design implications of the conclusion that in the absence of disturbances, an EMPC may in many cases pursue operation at an economically-optimal steady-state unless one of the following factors prevents it from doing so: A) short prediction horizon and sampling period lengths leading to myopic EMPC behavior; B) an objective function which changes; C) constraints which vary over time so that the closed-loop state can sometimes access higher-profit regions of state-space without violating the constraints, but cannot do so for all times, or the closed-loop state otherwise cannot remain at a location within the feasible set corresponding to the highest profit for all times but which can be reached during operation.

3.1.2.1. Time-Varying Operation and Design Analysis A: Sampling Period and Prediction Horizon. One factor which can cause an EMPC to not locate a steady-state operating condition corresponding to the greatest profit within the feasible set would be if it does not predict far enough into the future (i.e., the combination of the prediction horizon and sampling period do not allow the EMPC to see how it could reach the best operating point in the feasible region, so that it has difficulty to locate such a point). In addition, it may be possible that if an EMPC is desired to be used but the prediction horizon is too short, a traditional MPC may out-perform the EMPC for that same prediction horizon; therefore, if there are significant computational limitations known at the design stage, it may be necessary before seeking to find the optimal design to compare the EMPC performance with the prediction horizon and sampling period length which can be used with the available computational power with a steady-state tracking controller with the same computation time to verify which is more profitable before selecting a controller with which to explore process design.

3.1.2.2. Time-Varying Operation and Design Analysis B: Objective Function Change Timescale.
In this section, we discuss the implications for process design of the use of EMPC in cases where
the objective function is time-varying. In such cases, it is possible that EMPC may out-perform a
traditional tracking MPC (e.g., Ellis and Christofides (2014)) due to its ability to account explicitly
for profits as the cost function changes, without being forced to track a steady-state, particularly
if the changes in the objective function occur before or shortly after the closed-loop state shows
steady-state behavior with respect to a given objective function (i.e., the controller operates in a
transient fashion during a significant fraction of the time of operation). When the objective function
is time-varying, changes in the process design can change the character of the trajectories which an
EMPC would compute. To demonstrate this, we again consider the system of Eqs. 11-12, but this
time under an EMPC with the following objective function:

$$\int_{t_k}^{t_{k+N}} [10k_0 e^{-\frac{E}{RT(\tau)}} C_A(\tau)^2 - A(\tau) C_{A0}(\tau)] \, d\tau \tag{25}$$

where the first term represents revenue, and the second reflects operating costs (considered to
be related to costs of feedstock). A is either 0 or 100. For the process in Section 3.1, different
economically-optimal steady-states are associated with each value of A in Eq. 25. Specifically,
fmincon was utilized to locate a (locally) economically optimal steady-state with respect to the
stage cost of Eq. 25 for $A = 0$ and for $A = 100$. The steady-state optimization problem was
defined by maximizing Eq. 25 subject to the requirement that the steady-state dynamic model of
Eqs. 11-12 must be satisfied, with the inputs within the input bounds, and C_A and T within bounds
as well. Specifically, fmincon was utilized with the initial guesses of the decision variables (which
are steady-state values of C_A, T, C_{A0} and Q) being C_{As}, T_s, C_{A0s}, and Q_s from Section 3.1, lower
bounds on the values of these decision variables as 0.5 kmol/m^3, -5×10^5 kJ/h, 0 kmol/m^3, and
5 K, respectively, and upper bounds on these decision variables of 7.5 kmol/m^3, 5×10^5 kJ/h, 5
kmol/m^3, and 495 K. The problem was solved in MATLAB R2016a on a desktop Intel(R) Xeon(R)
CPU E-3 1240 v5. The optimal steady-state when $A = 0$ is $C_{A1s} = 0.86$ kmol/m^3, $T_{1s} = 495.00$ K,
$C_{A01s} = 7.50$ kmol/m^3, and $Q_{1s} = -156.11$ MJ/h, and the optimal steady-state when $A = 100$ is
$C_{A2s} = 0.19$ kmol/m^3, $T_{2s} = 495$ K, $C_{A02s} = 0.50$ kmol/m^3, and $Q_{2s} = 207.23$ MJ/h.

To demonstrate an interaction between process design and EMPC behavior, an EMPC was developed that optimizes the objective function in Eq. 25, subject to the constraint $T \leq 495$ K (enforced at the end of every integration step), as well as the bounds on the inputs ($0.5 \leq C_{A0} \leq 7.5$ kmol/m^3 and $-5.0 \times 10^5 \leq Q \leq 5.0 \times 10^5$ kJ/h). The model of Eqs. 11-12 was integrated using the Explicit Euler numerical integration method, with an integration step of 10^{-4} h. The optimization problems were solved using Ipopt Wächter and Biegler (2006) with automatic differentiation using ADOL-C Walther and Griewank (2009) on a desktop Intel(R) Xeon(R) CPU E-3 1240 v5 and with an Ipopt tolerance of 10^{-6}. Figs. 13-14 show the state and input trajectories of the process under the EMPC with A switching between 0 and 100 every 0.2 h. Each time A switches, the EMPC begins to track a new steady-state. To see the impact of process design on the EMPC's behavior, we consider also a case where the process design from Section 3.1 is modified so that $F = 1$ m^3/h and $V = 5$ m^3. In this case, the optimal steady-states for the steady-state optimization problem determined from fmincon occur for $A = 0$ at $C_{A1s} = 0.18$ kmol/m^3, $T_{1s} = 495.00$ K, $C_{A01s} = 7.50$ kmol/m^3, and $Q_{1s} = -39.13$ MJ/h and for $A = 100$ at $C_{A2s} = 0.05$ kmol/m^3, $T_{2s} = 495$ K, $C_{A02s} = 0.50$ kmol/m^3, and $Q_{2s} = 39.81$ MJ/h. From Figs. 13-14, it can be seen that changing the process design significantly impacted the EMPC's behavior by causing it to drive the closed-loop state to different economically-optimal steady-states than before over time. This highlights the concept of a sequential design framework described above, where the EMPC is designed before the process, and then changes in the process design are used by the EMPC to compute economically-optimal trajectories, but compared to designing, for example, an MPC to economically optimize process operation with each design, a benefit of using EMPC here is that it was not necessary to re-determine the steady-state each time that the process design changed (though this would not be the case for all EMPC designs, as many are designed around a steady-state), or to tune weighting matrices in an objective function. Rather, the EMPC was able to locate the economically-optimal trajectories for each design itself.

Another observation that can be made regarding the change in the design in Figs. 13-14 is that the design with $F = 1$ m^3/h has a lessened magnitude of variation in the concentration between changes in A because for that design, the optimal steady-states corresponding to each value of
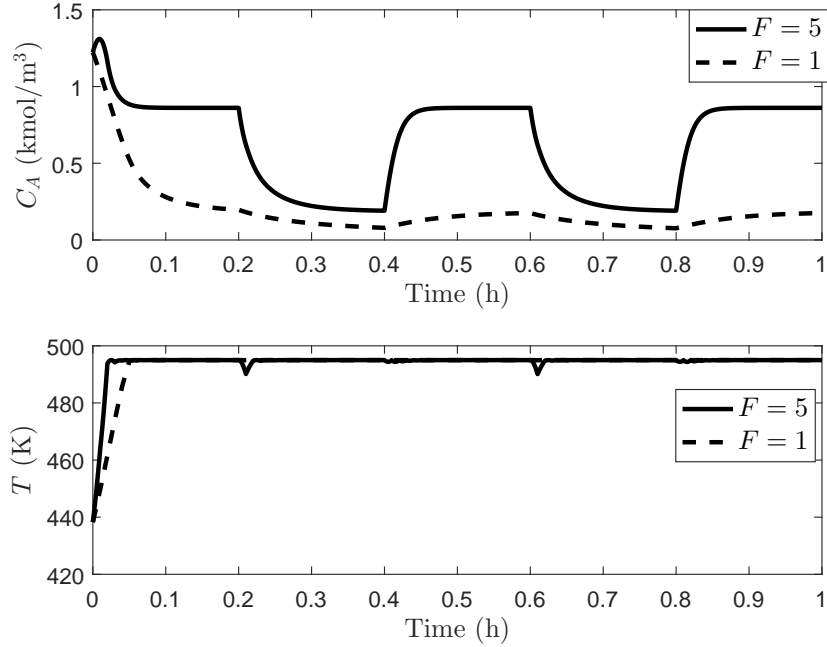
Figure 13: State trajectories under EMPC with the objective function of Eq. 25 where A changes every 0.2 h and either the process design with $F = 5$ m^3/h and $V = 1$ m^3 is used (labeled with "$F = 5$" on the legend) or the design with $F = 1$ m^3/h and $V = 5$ m^3 is used (labeled with "$F = 1$" on the legend).
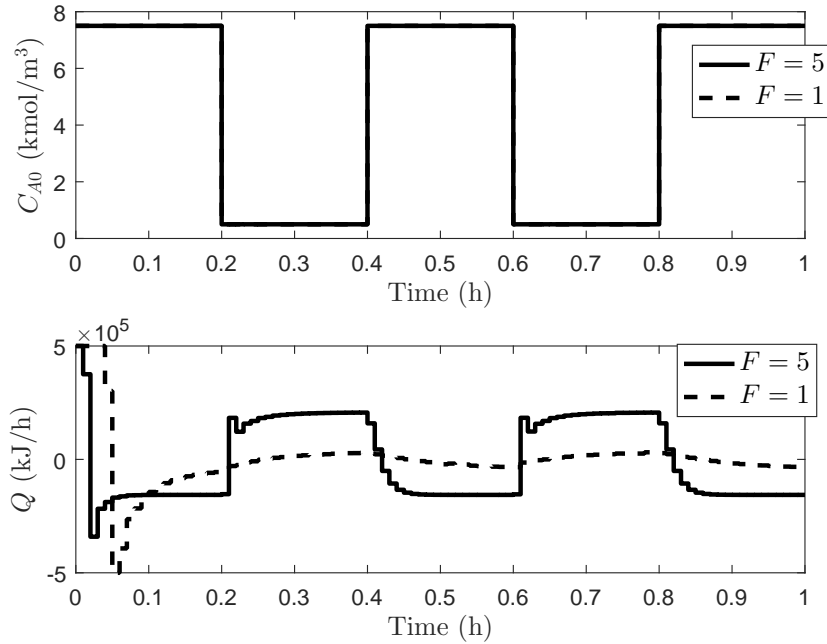
Figure 14: Input trajectories under EMPC with the objective function of Eq. 25 where A changes every 0.2 h and either the process design with $F = 5$ m^3/h and $V = 1$ m^3 is used (labeled with "$F = 5$" on the legend) or the design with $F = 1$ m^3/h and $V = 5$ m^3 is used (labeled with "$F = 1$" on the legend).

A have values of C_A that are not as far apart from one another as when $F = 5$ m^3/h. This again suggests a potential use of a simultaneous process and EMPC design framework. Specifically, it suggests that the design with $F = 1$ m^3/h may create less significant variations over time in concentration for processes further downstream, while still optimizing economics as the feedstock cost changes over time, than if the design with $F = 5$ m^3/h was chosen, which could be beneficial if it is desired to not account for the downstream process design and constraints for that part of the process in the EMPC. However, the total profit over 1 h of operation with $F = 5$ m^3/h is higher than that when $F = 1$ m^3/h; specifically, when $F = 5$ m^3/h, the time integral of the stage cost of Eq. 25 over 1 h of operation is 187.53, whereas with $F = 1$ m^3/h, it is -0.51 (reflecting profit losses). Finally, the consistent transient behavior with $F = 1$ m^3/h illustrates the concept that an EMPC may be considered for processes that do not consistently operate at steady-state, so that simulating the process behavior under the EMPC (rather than assuming that steady-state behavior will be achieved and determining the best designs for handling steady-states of operation) may be important for understanding the nature of the state trajectories and profits under different design scenarios under this type of controller.

3.2. Time-Varying Operation and Design Analysis C: Prevention of Optimal Steady-State Behavior

We here discuss further the simulation in Section 3.1.1.3 to demonstrate the concept that if at some point in time, the feasible region includes an optimal operating condition at which the closed-loop state cannot remain for all later times, this could be a case where EMPC may be utilized to attempt to optimize profits over time. For example, the EMPC designs in Section 3.1.1.1 created temperature profiles at the z = 0 position on the heat exchanger hot side that, after an initial transient, became an approximately constant value (Fig. 6). However, in Section 3.1.1.3, a time-varying operating condition was set up using the material constraint. In summary, in this example, a process constraint caused a different character of the trajectories under EMPC than if that constraint was not present. Potentially, there could be designs where the dynamics of the process itself prevent the closed-loop state from staying at a given state in the feasible set for all times (e.g., if a system experiences switches in its dynamic model after certain conditions are met which could be met during operation). However, we can also tie a constraint such as the material

constraint to the process dynamics more directly as well. Specifically, if a process is being designed for a future of operation under EMPC, it is possible to determine, by trading off operating costs (including, for example, feedstock cost) and capital costs (including storage vessels for the feedstock, for example) with revenue under EMPC, what the upper bound on the amount of available material should be. In such a process, initially, the feasible set could be set based on safety criteria; then, a material constraint could be added where the upper bound M_{ub} on the feedstock is a decision variable for a simultaneous design and control problem in which the optimization problem of Eq. 9 is seeking to find the process design variables and the controller decision variable M_{ub} that optimize the profits over time, including capital and operating costs when compared with revenue. If the feedstock storage facilities are cheap and do not need to be considered at the design stage in order to find the optimal process design, it would be possible to perform a sequential design in which there is no upper bound on the feedstock and the EMPC is allowed to cause the process to operate at any optimal operating condition in the safety-based feasible set, regardless of how much feedstock it uses (depending on the other constraints, this could be an optimal steady-state condition).

Remark 9. *The type of constraint examined in this section has been a primary motivator for the consideration of time-varying operation in the literature (e.g., Lee and Bailey (1980)). The above analysis highlights that considering feedstock constraints or other constraints which vary over time and restrict the feasible region may be beneficial at the design stage for attempting to evaluate whether time-varying operation of a process caused by such a constraint in the controller (and the subsequently less intuitive control designs and control actions) is more profitable than operating at a steady-state with more feedstock use allowed.*

4. Simultaneous Process and EMPC Design: Suggestions for Decision Variables in the Presence of Disturbances

The results of the prior sections focused on the absence of disturbances; in this section, we use the insights gained above to suggest which decision variables of an EMPC might be reasonable to look at in the presence of disturbances. First, we note that the prediction horizon and sampling period may play a role in achieving the highest profitability of the process in the presence of

disturbances, impacting the choice of the optimal process inputs, where different inputs acting on the same nonlinear process can produce different profits and degrees of constraint satisfaction. This highlights that N and/or Δ might be candidate controller decision variables in a simultaneous process and EMPC design framework in the presence of disturbances if a bound was placed on the allowable computation time of the controller. As for other simultaneous process and design works Yuan et al. (2012), control law factors influencing the satisfaction of constraints within the EMPC could serve as decision variables of the control law formulation. Potentially, these could have a character similar to that in Section 3.1.1.2, where to ensure that the process design requirement was met, a constraint was added to the controller that was used to attempt to ensure that the process design constraint was met at all times. In the presence of disturbances, a similar concept could be explored, where a controller parameter that impacts how close the closed-loop state comes under the computed control actions in the presence of disturbances to violating process constraints could be introduced and tuned to attempt to still allow the EMPC to have the greatest flexibility to make profit while ensuring that even in the presence of disturbances, process constraints would not be violated with the resulting control law. It is noted that this thinking is a departure from the sequential framework suggested in this paper without disturbances for EMPC and process design. Specifically, in the absence of disturbances, it was suggested that EMPC be equipped with complete knowledge of the process such that it is not necessary to have any type of "pseudo" constraint with a controller design variable being tuned by a simultaneous process and EMPC design algorithm because EMPC has the flexibility to be made aware of any objective function, model, and constraints of the process. The "pseudo" constraint was utilized when it was desired to not make the controller aware of the details of the whole process. In the presence of disturbances, however, EMPC no longer fully has this power; there are aspects of the process that are considered to be unknown, such that even the power of the controller to incorporate the model, constraints, and objective function does not overcome the potential need to tune parameters of the controller that can impact whether constraints of the process could be violated.

A consideration in this regard is that the EMPC could itself become infeasible if it includes hard constraints in the presence of disturbances. One idea could be to attempt to enforce a constraint

via soft constraints, and then to use the simultaneous control and process design framework to tune the bound utilized in setting the soft constraint appropriately. This is exemplified by returning once again to the process and controller in Section 3.1.1.2, but this time in the presence of disturbances, so that instead of enforcing a hard upper bound on temperature (to avoid potential infeasibility of the hard constraint in the controller), a soft constraint is imposed. Specifically, the decision variable s_d is introduced, and the objective function becomes Eq. 15 multiplied by 27.56 plus $10s_d^2$. The temperature constraint is modified to be $T - T_{ub} \leq s_d$. Bounded Gaussian white noise is added to the process model of Eqs. 11-12, with w_1 added to the right-hand side of Eq. 11 and w_2 added to the right-hand side of Eq. 12, with a standard deviation for w_1 of 30, and a standard deviation for w_2 of 3200 ($|w_1| \leq 90$ kmol/m^3 h and $|w_2| \leq 9600$ K/h). The function randn, seeded with rng, was utilized to generate the numbers, and then they were clipped at their bounds if the number generated exceeded its bound (simulations were run in MATLAB R2016b on a Lenovo model 80XN x64-based ideapad 320). In this case, with the seed of 10 to rng and $T_{ub} = 490$ K, the maximum temperature reached on the cold side of the heat exchanger in 0.5 h of operation was 2.1478 K above the initial steady-state value, which would violate the assumed 2 K temperature constraint but allowed a profit of 453.40 to be obtained. In contrast, if T_{ub} is decreased to 480 K, for the same disturbance trajectories, the maximum temperature reached on the cold side of the heat exchanger is only 1.77 K above the steady-state value, but the profit is reduced to 445.33. The tradeoff between meeting the temperature constraint and enhancing profits, under all possible realizations of the disturbances, and considering how the design of the process impacts the disturbance magnitude in the CSTR, could be optimized via a simultaneous process and EMPC design framework.

Stability theory for EMPC in the presence of disturbances may also be used to help to select controller design variables that are impacted by the magnitude of the disturbances, but which also impact profitability. For example, for LEMPC, the value of ρ_e should be made smaller when disturbances are larger to guarantee that the closed-loop state is maintained in Ω_ρ Heidarinejad et al. (2012). However, larger values of ρ_e may enhance profits by making the region Ω_{ρ_e}, within which the economics-based objective function is optimized (Eq. 8a), larger. A value of ρ_e that would guarantee closed-loop stability can be defined in terms of a number of functions and parameters

that are difficult to determine in practice Heidarinejad et al. (2012); a simultaneous process and control design framework could provide a means for tuning ρ_e, and for assessing how process designs would impact the conservatism of that parameter and therefore the profitability of the EMPC of Eqs. 6 and 8. Therefore, ρ_e is a potential control design decision variable for LEMPC that could be adjusted in the presence of disturbances. Potentially, a simultaneous control and process design framework could help industrial practitioners to address the question of how to operate as close to the limits of safe operation, when that is most profitable, as possible, without losing safety. It may provide a means for addressing how to design EMPC's to respect both safety and profitability objectives, even with uncertainty.

5. Conclusions

This work aimed to provide a preliminary investigation into how controller and process design decisions interact under an EMPC operating policy and to show whether or not a simultaneous process and EMPC design framework is necessary for processes in the absence of disturbances. In particular, we noted that for processes operated under EMPC in the absence of disturbances, a sequential approach for designing processes and EMPC may be adequate for achieving the most profitable design due to the EMPC capability to directly optimize the process economics on-line (i.e., there is no need to tune controller decision variables to better reflect process economics unless an attempt is being made to utilize the design and auxiliary constraints in the controller to reduce the need to incorporate as much information about the design in the control law (which has the potential to increase computation time)). We discussed how design is related to the major factors which affect whether an EMPC promotes time-varying or steady-state operation in the absence of disturbances, and suggested several controller design variables which could be decision variables for a simultaneous process and EMPC design framework in the presence of disturbances.

Challenges that could be explored for simultaneous design and control for EMPC, in the presence of disturbances, in the future include: 1) Utilizing imperfect models when making the design decisions. Appropriate process models (e.g., first-principles model) must be available to allow an effective assessment of the impact of process and controller decision variables on overall performance

and operating requirements. At the design stage, data for modeling purposes may not be sufficient. 2) Making the simultaneous design and control framework tractable. It may be challenging to solve a bilevel optimization problem to global optimality for a large design search space, especially if the prediction horizon and therefore the long-term dynamic behavior of the process under EMPC is taken into account.

Overall, the results suggest that the major benefit of considering the implications of process design for EMPC design, and vice versa, are that a framework for addressing both designs at once may help to relieve a steady-state mentality in the design process. The analysis above for the simultaneous design problem in the absence of disturbances bears many similarities to the general discussion about whether EMPC will actually operate a process in a steady-state fashion; the major claims in the literature have been that even if it does so, part of the benefit of using such a general controller is that it reduces the human guesswork in trying to figure out whether steady-state or time-varying operation will be most suitable *a priori*, and relies on an optimization algorithm to figure out the optimal situation. The use of an appropriately formulated EMPC and process co-design framework can similarly aid in figuring out what the optimal way to design a process for operation under EMPC is. It may help to identify new use cases where EMPC out-performs steady-state operation in ways that had not previously been considered, and may also be used in comparing designs and expected behavior and profitability under the design under both EMPC and under MPC.

6. Acknowledgements

Literature Cited

Adeodu, O., Chmielewski, D.J., 2018. A two-stage procedure for the optimal sizing and placement of grid-level energy storage. Computers & Chemical Engineering 114, 265–272.

Alanqar, A., Ellis, M., Christofides, P.D., 2015. Economic model predictive control of nonlinear process systems using empirical models. AIChE Journal 61, 816–830.

Bahakim, S.S., Ricardez-Sandoval, L.A., 2014. Simultaneous design and MPC-based control for dynamic systems under uncertainty: A stochastic approach. Computers & Chemical Engineering 63, 66–81.

Baldea, M., Edgar, T.F., 2018. Dynamic process intensification. Current Opinion in Chemical Engineering 22, 48–53. Biotechnology and Bioprocess Engineering.

Baldea, M., Touretzky, C.R., 2013. Nonlinear model predictive control of energy-integrated process systems. Systems & Control Letters 62, 723–731.

Bansal, V., Perkins, J., Pistikopoulos, E., Ross, R., van Schijndel, J., 2000. Simultaneous design and control optimisation under uncertainty. Computers & Chemical Engineering 24, 261–266.

Bansal, V., Perkins, J.D., Pistikopoulos, E.N., 2002. A case study in simultaneous design and control using rigorous, mixed-integer dynamic optimization models. Industrial & Engineering Chemistry Research 41, 760–778.

Brengel, D., Seider, W., 1992. Coordinated design and control optimization of nonlinear processes. Computers & Chemical Engineering 16, 861–886.

Budman, H., Silveston, P., 2008. Control of periodically operated reactors. Chemical Engineering Science 63, 4942–4954.

Carrasco, J.C., Lima, F.V., 2017. An optimization-based operability framework for process design and intensification of modular natural gas utilization systems. Computers & Chemical Engineering 105, 246–258.

Christofides, P., F. Davis, J., H. El-Farra, N., Clark, D., R. D. Harris, K., N. Gipson, J., 2007. Smart plant operations: Vision, progress and challenges. AIChE Journal 53, 2734–2741.

Davis, J., Edgar, T., Graybill, R., Korambath, P., Schott, B., Swink, D., Wang, J., Wetzel, J., 2015. Smart manufacturing. Annual Review of Chemical and Biomolecular Engineering 6, 141–160.

Diehl, M., Amrit, R., Rawlings, J.B., 2011. A Lyapunov function for economic optimizing model predictive control. IEEE Transactions on Automatic Control 56, 703–707.

Douglas, J.M., 1967. Periodic reactor operation. Industrial & Engineering Chemistry Process Design and Development 6, 43–48.

Durand, H., 2019. On accounting for equipment-control interactions in economic model predictive control via process state constraints. Chemical Engineering Research and Design 144, 63–78.

Ellis, M., Christofides, P.D., 2014. Economic model predictive control with time-varying objective function for nonlinear process systems. AIChE Journal 60, 507–519.

Ellis, M., Durand, H., Christofides, P.D., 2014. A tutorial review of economic model predictive control methods. Journal of Process Control 24, 1156–1178.

Flores-Tlacuahuac, A., Biegler, L.T., 2005. A robust and efficient mixed-integer non-linear dynamic optimization approach for simultaneous design and control, in: Puigjaner, L., Espuña, A. (Eds.), European Symposium on Computer-Aided Process Engineering-15, 38th European Symposium of the Working Party on Computer Aided Process Engineering. Elsevier. volume 20 of *Computer Aided Chemical Engineering*, pp. 67–72.

Flores-Tlacuahuac, A., Biegler, L.T., 2007. Simultaneous mixed-integer dynamic optimization for integrated design and control. Computers & Chemical Engineering 31, 588–600.

Francisco, M., Revollar, S., Vega, P., Lamanna, R., 2009. Simultaneous synthesis, design and control of processes using model predictive control. IFAC Proceedings Volumes 42, 863–868. 7th IFAC Symposium on Advanced Control of Chemical Processes.

Gazzaneo, V., Lima, F.V., 2019. Multilayer operability framework for process design, intensification, and modularization of nonlinear energy systems. Industrial & Engineering Chemistry Research 58, 6069–6079.

Georgiadis, M.C., Schenk, M., Pistikopoulos, E.N., Gani, R., 2002. The interactions of design control and operability in reactive distillation systems. Computers & Chemical Engineering 26, 735–746.

Gutierrez, G., Ricardez-Sandoval, L., Budman, H., Prada, C., 2014. An MPC-based control structure selection approach for simultaneous process and control design. Computers & Chemical Engineering 70, 11–21.

Heidarinejad, M., Liu, J., Christofides, P.D., 2012. Economic model predictive control of nonlinear process systems using Lyapunov techniques. AIChE Journal 58, 855–870.

Hoffmann, C., Esche, E., Repke, J.U., 2019. Integration of design and control based on large-scale nlp formulations and an optimal economic nmpc, in: Muñoz, S.G., Laird, C.D., Realff, M.J. (Eds.), Proceedings of the 9th International Conference on Foundations of Computer-Aided Process Design. Elsevier. volume 47 of *Computer Aided Chemical Engineering*, pp. 125–130.

Huang, R., Harinath, E., Biegler, L., 2011. Lyapunov stability of economically oriented NMPC for cyclic processes. Journal of Process Control 21, 501–509.

Isafiade, A., Fraser, D., 2010. Interval based MINLP superstructure synthesis of heat exchanger networks for multi-period operations. Chemical Engineering Research and Design 88, 1329–1341.

Kookos, I.K., Perkins, J.D., 2001. An algorithm for simultaneous process design and control. Industrial & Engineering Chemistry Research 40, 4079–4088.

Kyriakides, A.S., Zarogiannis, T., Seferlis, P., 2017. Integrated process design and control: A review of the current state-of-the-art and research challenges. Chemical Engineering Transactions 61, 1417–1422.

Lee, C., Bailey, J.E., 1980. Modification of consecutive-competitive reaction selectivity by periodic operation. Industrial & Engineering Chemistry Process Design and Development 19, 160–166.

Lin, Y., Sontag, E.D., 1991. A universal formula for stabilization with bounded controls. Systems & Control Letters 16, 393–397.

Mayne, D., Rawlings, J., Rao, C., Scokaert, P., 2000. Constrained model predictive control: Stability and optimality. Automatica 36, 789–814.

Mohideen, M., Perkins, J., Pistikopoulos, E., 1996a. Optimal synthesis and design of dynamic systems under uncertainty. Computers & Chemical Engineering 20, S895–S900.

Mohideen, M.J., Perkins, J.D., Pistikopoulos, E.N., 1996b. Optimal design of dynamic systems under uncertainty. AIChE Journal 42, 2251–2272.

Moulijn, J.A., Stankiewicz, A., Grievink, J., Górak, A., 2008. Process intensification and process systems engineering: A friendly symbiosis. Computers & Chemical Engineering 32, 3–11.

Ogunnaike, B.A., Ray, W.H., 1994. Process Dynamics, Modeling, and Control. Oxford University Press, New York, NY.

Perkins, J., Walsh, S., 1996. Optimization as a tool for design/control integration. Computers & Chemical Engineering 20, 315–323.

Pistikopoulos, E.N., Diangelakis, N.A., 2016. Towards the integration of process design, control and scheduling: Are we getting closer? Computers & Chemical Engineering 91, 85–92.

Qin, S.J., Badgwell, T.A., 2003. A survey of industrial model predictive control technology. Control Engineering Practice 11, 733–764.

R Vinson, D., Georgakis, C., 2000. A new measure of process output controllability. Journal of Process Control 10, 185–194.

Rafiei, M., Ricardez-Sandoval, L.A., 2020. New frontiers, challenges, and opportunities in integration of design and control for enterprise-wide sustainability. Computers & Chemical Engineering 132, 106610.

Rafiei-Shishavan, M., Mehta, S., Ricardez-Sandoval, L.A., 2017. Simultaneous design and control under uncertainty: A back-off approach using power series expansions. Computers & Chemical Engineering 99, 66 – 81.

Rawlings, J.B., 2000. Tutorial overview of model predictive control. IEEE Control Systems Magazine 20, 38–52.

Rawlings, J.B., Angeli, D., Bates, C.N., 2012. Fundamentals of economic model predictive control, in: Proceedings of the Conference on Decision and Control, Maui, Hawaii. pp. 3851–3861.

Ricardez-Sandoval, L., Budman, H., Douglas, P., 2009. Integration of design and control for chemical processes: A review of the literature and some recent results. Annual Reviews in Control 33, 158–171.

Ricardez-Sandoval, L., Douglas, P., Budman, H., 2011. A methodology for the simultaneous design and control of large-scale systems under process parameter uncertainty. Computers & Chemical Engineering 35, 307–318.

Ross, R., Bansal, V., Perkins, J., Pistikopoulos, E., Koot, G., van Schijndel, J., 1999. Optimal design and control of an industrial distillation system. Computers & Chemical Engineering 23, S875–S878.

Sakizlis, V., Perkins, J.D., Pistikopoulos, E.N., 2004. Recent advances in optimization-based simultaneous process and control design. Computers & Chemical Engineering 28, 2069–2086.

Sanchez-Sanchez, K.B., Ricardez-Sandoval, L.A., 2013. Simultaneous design and control under uncertainty using model predictive control. Industrial & Engineering Chemistry Research 52, 4815–4833.

Seider, W.D., Lewin, D.R., Seader, J.D., Widagdo, S., Gani, R., Ming, N.G., 2017. K. product and process design principles: Synthesis, analysis and evaluation.

Silveston, P., Hudgins, R.R., Renken, A., 1995. Periodic operation of catalytic reactors introduction and overview. Catalysis Today 25, 91–112.

Skiborowski, M., 2018. Process synthesis and design methods for process intensification. Current Opinion in Chemical Engineering 22, 216–225.

Sánchez-Sánchez, K., Ricardez-Sandoval, L., 2013. Simultaneous process synthesis and control design under uncertainty: A worst-case performance approach. AIChE Journal 59, 2497–2514.

Swartz, C.L., Kawajiri, Y., 2019. Design for dynamic operation - a review and new perspectives for an increasingly dynamic plant operating environment. Computers & Chemical Engineering 128, 329 – 339. URL: http://www.sciencedirect.com/science/article/pii/S0098135419300705, doi:https://doi.org/10.1016/j.compchemeng.2019.06.002.

T. Backx, O.B., Marquardt, W., 1998. Towards intentional dynamics in supply chain conscious process operations.

Wächter, A., Biegler, L.T., 2006. On the implementation of an interior-point filter line-search algorithm for large-scale nonlinear programming. Mathematical Programming 106, 25–57.

Walther, A., Griewank, A., 2009. Getting started with ADOL-C. Combinatorial scientific computing , 181–202.

Yuan, Z.h., Chen, B., Sin, G., Gani, R., 2012. State-of-the-art and progress in the optimization-based simultaneous design and control for chemical processes. AIChE Journal 58, 1640–1659.

Ziegler, J., Nichols, N., 1943. Process lags in automatic control circuits. Transactions ASME 65, 433–443.